

# DESIGNING OF TIME-FREQUENCY LOCALIZATION OPTIMIZED TWO-CHANNEL ORTHOGONAL WAVELET FILTER BANKS

*A Dissertation  
submitted in partial fulfillment of the requirements  
for the Degree of*

**Master of Technology**

*with  
specialization in*

**Electronic Systems**

*by*

**Saket Porwal  
(11307R006)**

Supervisor

**Prof. Vikram M. Gadre**



Department of Electrical Engineering  
Indian Institute of Technology, Bombay  
Powai, Mumbai - 400 076.

**2014**

*Dedicated to  
my parents and my angel Parul*

## **Declaration of the Academic Ethics**

I declare that this written submission represents my ideas in my own words and where others' ideas or words have been included, I adequately cited and referenced the original sources. I declare that I have properly and accurately acknowledged all sources used in the production of this thesis.

I also declare that I have adhered to all principles of academic honesty and integrity and have not misrepresented or fabricated or falsified any idea/ data/ fact/ source in my submission. I understand that any violation of the above will be a cause for disciplinary action by the Institute and can also evoke penal action from the sources which have not been properly cited or from whom proper permission has not been taken when needed.

Date: .....

Saket Porwal

(Roll No. 11307R006)

## ACKNOWLEDGEMENTS

First and foremost, I would like to express my gratitude to my guide Prof. V.M. Gadre who with his profound experience and never ending enthusiasm provided constant support and guidance to my dissertation.

I would like to heartily thank Mr. Manish Sharma for his support and encouragement. He solved all kinds of doubts and brought immense clarity to my concepts. He has been a wonderful friend and guide to me.

I would like to thank Mr. Ankit Bhurane, Mr. Sujath Nair and Mr. Akhil Lalwani. Many times their cross-questions made me go through the basics, which helped me a lot.

I would like to thank my friend Ms. Deepti Panchratna whose support and encouragement helped me a lot in completion of my dissertation.

I acknowledge the *Bharti Centre for Communication, Department of Electrical Engineering, Indian Institute of Technology Bombay* for providing the financial support.

Finally, I would like to thank my parents and TIDSP lab mates, who provided the needed base to work conveniently.

## **Abstract**

A new framework has been devised to design a class of time-frequency localization optimized, orthogonal wavelet filter banks. Three design problems are proposed to design the optimal orthogonal filter banks. Semidefinite programming (SDP) is used to solve the three design problems. An analysis low-pass filter is first designed and the impulse response of the other members of the filter bank is computed employing the quadrature conjugate symmetry (CQ). The time-frequency localization based optimality criterion is used to design the filter bank. The objective function taken in Design Problem 1 is the convex combination of the time variance and the frequency variance (CCTFV) of the impulse response of the analysis low-pass filter, which is minimized subjected to double shift orthogonality and vanishing moment constraints. In Design Problem 2, the time variance of the analysis filter is minimized after fixing the frequency variance to a constant value, whereas in Design Problem 3, the frequency variance is minimized after fixing the time variance to a constant value. A few design examples for three design problems are discussed in the report.

# Contents

<b>1</b>	<b>Introduction</b>	<b>1</b>
1.1	Perfect Reconstruction Filter Banks . . . . .	1
1.1.1	Orthogonal Filter Banks . . . . .	2
1.1.2	Biorthogonal Filter Banks . . . . .	3
1.2	Optimality Criterion . . . . .	4
1.3	Semidefinite Programming . . . . .	6
1.4	Organization of the Report . . . . .	8
<b>2</b>	<b>Literature Survey</b>	<b>9</b>
2.1	Time-Frequency Uncertainty . . . . .	9
2.1.1	Uncertainty in Continuous-Time Domain . . . . .	9
2.1.2	Uncertainty in Discrete-Time Domain . . . . .	11
2.2	Earlier Work on Time Frequency Localizarion Based Filters and Filter Banks . . . . .	12
<b>3</b>	<b>The Devised Framework</b>	<b>14</b>
3.1	Time Variance . . . . .	15
3.2	Frequency Variance . . . . .	17
3.3	The CCTFV . . . . .	19
3.4	The Double Shift Orthogonality . . . . .	20
3.4.1	Formulation of ACF . . . . .	20
3.5	Vanishing Moments . . . . .	22
3.6	Filter Norm . . . . .	24
3.7	Iterative SDP . . . . .	25
3.8	The Design Problems . . . . .	26
3.8.1	The Design Problem 1 . . . . .	26
3.8.2	The Design Problem 2 . . . . .	27
3.8.3	The Design Problem 3 . . . . .	28
3.8.4	Constraints on Design Parameters . . . . .	29
3.9	Construction of Wavelets . . . . .	30
3.10	Design Flow . . . . .	30

---

<b>4</b>	<b>Design Examples</b>	<b>33</b>
4.1	Design Examples for Design Problem 1 . . . . .	34
4.1.1	Design Example 1 . . . . .	34
4.1.2	Design Example 2 . . . . .	35
4.1.3	Design Example 3 . . . . .	35
4.1.4	Design Example 4 . . . . .	38
4.1.5	Design Example 5 . . . . .	41
4.2	Design Examples for Design Problem 2 and 3 . . . . .	41
4.2.1	Design Example 6 . . . . .	41
4.2.2	Design Example 7 . . . . .	43
4.2.3	Design Example 8 . . . . .	43
4.3	Time-Frequency properties of obtained filters . . . . .	48
<b>5</b>	<b>Conclusion and Future Work</b>	<b>52</b>
	<b>Bibliography</b>	<b>54</b>
	<b>Appendices</b>	<b>58</b>
<b>A</b>		<b>59</b>
A.1	Derivation of Matrix Formulation for Frequency Variance . . . . .	59

# List of Figures

1.1	Two-channel 1D filter bank . . . . .	2
3.1	Flow chart to design the optimal filter bank . . . . .	32
4.1	Example 1 . . . . .	36
(a)	Plot of $ H_0(\omega) $ and $ H_1(\omega) $ for Example-1 . . . . .	36
(b)	Plot of $R(\omega)$ and $R(\omega + \pi)$ for Example-1 . . . . .	36
(c)	Analysis Scaling Function for Example-1 . . . . .	36
(d)	Analysis Wavelet for Example-1 . . . . .	36
(e)	Pole Zero Plot for Example-1 . . . . .	36
4.2	Example 2 . . . . .	37
(a)	Plot of $ H_0(\omega) $ and $ H_1(\omega) $ for Example-2 . . . . .	37
(b)	Plot of $R(\omega)$ and $R(\omega + \pi)$ for Example-2 . . . . .	37
(c)	Analysis Scaling Function for Example-2 . . . . .	37
(d)	Analysis Wavelet for Example-2 . . . . .	37
(e)	Pole Zero Plot for Example-2 . . . . .	37
4.3	Example 3 . . . . .	39
(a)	Plot of $ H_0(\omega) $ and $ H_1(\omega) $ for Example-3 . . . . .	39
(b)	Plot of $R(\omega)$ and $R(\omega + \pi)$ for Example-3 . . . . .	39
(c)	Analysis Scaling Function for Example-3 . . . . .	39
(d)	Analysis Wavelet for Example-3 . . . . .	39
(e)	Pole Zero Plot for Example-3 . . . . .	39
4.4	Example 4 . . . . .	40
(a)	Plot of $ H_0(\omega) $ and $ H_1(\omega) $ for Example-4 . . . . .	40
(b)	Plot of $R(\omega)$ and $R(\omega + \pi)$ for Example-4 . . . . .	40
(c)	Analysis Scaling Function for Example-4 . . . . .	40
(d)	Analysis Wavelet for Example-4 . . . . .	40
(e)	Pole Zero Plot for Example-4 . . . . .	40
4.5	Example 5 . . . . .	42
(a)	Plot of $ H_0(\omega) $ and $ H_1(\omega) $ for Example-5 . . . . .	42
(b)	Plot of $R(\omega)$ and $R(\omega + \pi)$ for Example-5 . . . . .	42
(c)	Analysis Scaling Function for Example-4 . . . . .	42
(d)	Analysis Wavelet for Example-4 . . . . .	42
(e)	Pole Zero Plot for Example-5 . . . . .	42



4.6	Example 6 . . . . .	44
(a)	Plot of $ H_0(\omega) $ and $ H_1(\omega) $ for Example-6 . . . . .	44
(b)	Plot of $R(\omega)$ and $R(\omega + \pi)$ for Example-6 . . . . .	44
(c)	Analysis Scaling Function for Example-6 . . . . .	44
(d)	Analysis Wavelet for Example-6 . . . . .	44
(e)	Pole Zero Plot for Example-6 . . . . .	44
4.7	Example 7 . . . . .	45
(a)	Plot of $ H_0(\omega) $ and $ H_1(\omega) $ for Example-7 . . . . .	45
(b)	Plot of $R(\omega)$ and $R(\omega + \pi)$ for Example-7 . . . . .	45
(c)	Analysis Scaling Function for Example-7 . . . . .	45
(d)	Analysis Wavelet for Example-7 . . . . .	45
(e)	Pole Zero Plot for Example-7 . . . . .	45
4.8	Time-Frequency Localization Measures. . . . .	46
4.9	Example 8 . . . . .	47
(a)	Plot of $ H_0(\omega) $ and $ H_1(\omega) $ for Example-8 . . . . .	47
(b)	Plot of $R(\omega)$ and $R(\omega + \pi)$ for Example-8 . . . . .	47
(c)	Analysis Scaling Function for Example-8 . . . . .	47
(d)	Analysis Wavelet for Example-8 . . . . .	47
(e)	Pole Zero Plot for Example-8 . . . . .	47

# List of Tables

4.1	Time-Frequency properties of the analysis and synthesis LPF of Design Examples . . . . .	49
4.2	Filter Coefficients of Design Examples . . . . .	50
4.3	Filter Coefficients of Design Examples . . . . .	50
4.4	Filter Coefficients of Design Examples . . . . .	51

# Chapter 1

## Introduction

Wavelet transform is one of the most powerful tool that is used for multi-scale or multi-resolution analysis. Wavelet transform can be realized using filter banks by which a signal can be decomposed at different resolutions. The advantage of the wavelet in signal analysis is the simultaneous localization in the time as well as in frequency domain to a great extent. In the present work time-frequency localization is taken as an optimality criterion to design the orthogonal filter banks. We aim to design the time-frequency localization optimized filter banks employing a semidefinite programming based approach. This chapter gives the introduction to FIR filter banks along with the optimality criterion used to design the filter banks. We also discuss semidefinite programming (SDP), which is an optimization technique that has been employed to design the filter banks.

### 1.1 Perfect Reconstruction Filter Banks

A typical two-channel filter bank is shown in Fig. 1.1.  $H_0(z)$  and  $H_1(z)$  are analysis low-pass and high-pass filters, respectively, and  $F_0(z)$  and  $F_1(z)$  are synthesis low-pass and high-pass filters.

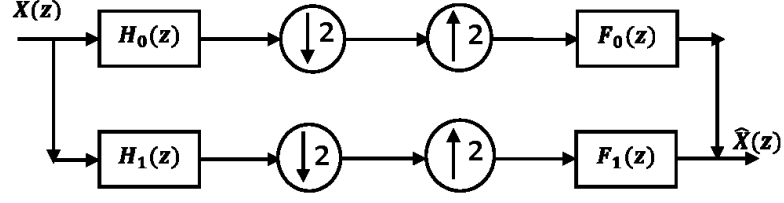


Figure 1.1: Two-channel 1D filter bank

### 1.1.1 Orthogonal Filter Banks

In the present work, we proposed three design problem to design time-frequency localization optimized orthogonal filter banks. In the very simple words, the design of orthogonal filter means to generate an even length sequence which is orthonormal to its even shifts, this orthonormality ensures the perfect reconstruction, i.e. the signal decomposed by an analysis filter bank can be reconstructed using the synthesis filter bank. The length of the filters of the orthogonal filter bank is even because the odd length orthogonal perfect reconstruction real valued filter bank is fundamentally not possible. Also a real valued perfect reconstruction symmetric orthogonal filter bank is not possible except for the 2 length length case [21].

To design orthogonal filter bank, the analysis low-pass filter is first designed. The other filters are then obtained employing conjugate quadrature symmetry. The impulse response of the analysis high-pass filter can be obtained as,

$$h_1(n) = (-1)^n h_0(M - n) \quad (1.1)$$

Where,  $M$  is an odd natural number such that,

$$h_0(n) = 0 \quad \forall n \in \{(n < 0) \cup (n > M)\}$$

Hence the length of the filter is

$$L = M + 1$$

The other members,  $f_0(n)$  and  $f_1(n)$  can be obtained as,

$$f_0(n) = h_0(M - n) \quad (1.2)$$

$$f_1(n) = h_1(M - n) \quad (1.3)$$

Equations 1.1 and 1.2 and 1.3 ensure the alias cancellation. In this manner all the four members of the filter banks are obtained.

### 1.1.2 Biorthogonal Filter Banks

The symmetric orthogonal filter banks are not possible, the same creates the need to design a biorthogonal filter bank, in which symmetry can be achieved and hence the linear phase [21]. Let  $h_0(n)$  and  $f_0(n)$  are the impulse response of the low-pass filter of the analysis and the synthesis filter bank respectively such that,

$$h_0(n) = 0 \quad \forall |n| > P \quad (1.4)$$

$$f_0(n) = 0 \quad \forall |n| > Q \quad (1.5)$$

The other members can be obtained using the following equations,

$$h_1(n) = (-1)^n f_0(n) \quad (1.6)$$

$$f_1(n) = (-1)^n h_0(n) \quad (1.7)$$

The above two equations ensure the alias cancellation condition. Defining the product filter,  $P(z) = H_0(z)F_0(z)$ , the PR condition can be expressed in  $z$ -domain as :

$$P(z) + P(-z) = 2 \quad (1.8)$$

It can be shown that the inverse  $Z$  transform of  $P(Z)$ ,  $p(n)$  is equal to zero at all even indices except  $n = 0$ . Such sequences are known as half-band sequences [26].

## 1.2 Optimality Criterion

The fundamental problem of time-frequency localization is that a signal cannot be localized in time and frequency simultaneously beyond a certain extent. There is a lower bound on the time-frequency measures. In the present work, we design the filter banks with time-frequency localization based optimality criterion. For the Design Problem 1, the objective function taken is the convex combination of the time variance,  $\sigma_n^2$  and the frequency variance,  $\sigma_\omega^2$  of the filter impulse response. In the whole report, we call this quantity **CCTFV** of the filter impulse response. M. Sharma et al. [18] took CCTFV as an objective function to design the biorthogonal filter bank. The following equations define the time and frequency variance [7, 8].

$$\begin{aligned}\sigma_n^2 &= \sum_n (n - n_0)^2 |h(n)|^2 \\ \sigma_\omega^2 &= \int_{\mathbb{R}} \omega^2 |H(\omega)|^2 d\omega\end{aligned}$$

Where  $H(\omega)$  is the DTFT of  $h(n)$  and  $n_0$  is the time center given as

$$n_0 = \sum_n n |h(n)|^2$$

CCTFV [18] of the filter with impulse response is given by,

$$\phi = \alpha \sigma_n^2 + (1 - \alpha) \sigma_\omega^2$$

where  $\alpha \in [0, 1]$

The Design Problem 1 uses CCTFV of the impulse response of the analysis low-pass filter as an objective function. Whereas in the Design Problem 2, we first fix the frequency variance to a constant value and then try to minimize the time variance of the analysis low-pass filter, the vice-versa of this is done in the Design Problem 3, i.e. we fixed time variance to a certain value and then the frequency variance is minimized. In all the three designs we try to optimize the

time-frequency localization uncertainty of the analysis filter.

The advantage of using CCTFV as an optimality criterion is that, the frequency and time variances are simultaneously reduced, unlike the time-frequency product (TFP) where we just know that the time-frequency product is reduced [18]. CCTFV provide a degree of freedom which is the value of  $\alpha \in [0, 1]$ , for example, if one wants to concentrate only on time variance, the value of  $\alpha$  can be set to unity. The CCTFV can not be minimized beyond a certain value. CCTFV has a lower bound [18]. It can simply be derived from the fact that the arithmetic mean (A.M.) of two real numbers is greater than the geometric mean (G.M.), mathematically,

$$\begin{aligned} \frac{\alpha\sigma_n^2 + (1-\alpha)\sigma_\omega^2}{2} &\geq \sqrt{\alpha\sigma_n^2(1-\alpha)\sigma_\omega^2} \\ \alpha\sigma_n^2 + (1-\alpha)\sigma_\omega^2 &\geq \sqrt{\alpha(1-\alpha)} 2\sigma_n\sigma_\omega \end{aligned} \quad (1.9)$$

Hence,

$$\Phi \geq \sqrt{\alpha(1-\alpha)} 2\sigma_n\sigma_\omega \quad (1.10)$$

The product of time-frequency variances for a low-pass sequence is bounded by  $\frac{1}{4}$  [7, 8] mathematically,

$$\begin{aligned} \sigma_n^2\sigma_\omega^2 &\geq \frac{1}{4} \\ \text{i.e. } \sigma_n\sigma_\omega &\geq \frac{1}{2} \end{aligned} \quad (1.11)$$

Hence, for the low-pass discrete sequences,

$$\Phi \geq \sqrt{\alpha(1-\alpha)} \quad (1.12)$$

The above inequality holds true for any kind of low-pass discrete sequence. In

general,

$$\sigma_n^2 \sigma_\omega^2 \geq \frac{1}{4} (1 - H(e^{j\pi}))^2 \quad (1.13)$$

Hence, for the sequences with  $H(e^{j\pi}) = 1$ , the following inequality holds,

$$\Phi \geq 0 \quad (1.14)$$

### 1.3 Semidefinite Programming

In the present work, we use semidefinite programming (SDP) [27] based approach to design the time-frequency localization optimized orthogonal filter banks. The double shift orthogonality constraints are fundamentally non-convex. The design problems proposed in the present have the form of the problem stated in Eq. 1.15. Let

$$\mathbf{x} = \begin{bmatrix} h_0(0) & h_0(1) & \dots & h_0(M-1) & h_0(M) \end{bmatrix}^T, \quad M \in \mathbb{N}$$

Where  $h(n)$  is the real valued impulse response of the analysis low-pass filter. It is important to note that  $\mathbf{x} \in \mathbb{R}^{M+1}$ . In general the orthogonal filter bank design problem can be stated as,

$$\begin{aligned} & \underset{\mathbf{x}}{\text{minimize}} && \mathbf{x}^T \mathbf{R} \mathbf{x} \\ & \text{subject to} && \mathbf{A} \mathbf{x} = \mathbf{0} \\ & && \mathbf{x}^T \mathbf{x} = 1 \\ & && \mathbf{x}^T \mathbf{\Theta}_{2k} \mathbf{x} = 0, \quad k = 1, 2, \dots, \frac{M-1}{2} \end{aligned} \quad (1.15)$$

Where  $\mathbf{x}^T \mathbf{R} \mathbf{x}$  is the objective function in quadratic form and  $\mathbf{A} \mathbf{x} = \mathbf{0}$  is the formulation of vanishing moments and  $\mathbf{x}^T \mathbf{\Theta}_{2k} \mathbf{x} = 0, \quad k = 1, 2, \dots, \frac{M-1}{2}$  is the formulation of double shift orthogonality constraints. All the formulations are explained in detail in Chapter 3. The problem stated by Eq. 1.15 is non-convex



because of the double shift orthogonality constraints. The same problem can be transformed to a convex problem using trace parameterization [3]. The problem (1.15) can be re-written as,

$$\begin{aligned}
& \underset{\mathbf{x}}{\text{minimize}} && \text{Tr}(\mathbf{R}\mathbf{x}\mathbf{x}^T) \\
& \text{subject to} && \mathbf{A}\mathbf{x}\mathbf{x}^T = \mathbf{0} \\
& && \text{Tr}(\mathbf{x}\mathbf{x}^T) = 1 \\
& && \text{Tr}(\mathbf{\Theta}_{2k}\mathbf{x}\mathbf{x}^T) = 0, \quad k = 1, 2, \dots, \frac{M-1}{2}
\end{aligned} \tag{1.16}$$

Introducing a new variable  $\mathbf{X} = \mathbf{x}\mathbf{x}^T$ . It is to be noted that matrix  $\mathbf{X}$  is a unity rank positive semidefinite matrix. The above problem can be re-written as,

$$\begin{aligned}
& \underset{\mathbf{X}}{\text{minimize}} && \text{Tr}(\mathbf{R}\mathbf{X}) \\
& \text{subject to} && \mathbf{A}\mathbf{X} = \mathbf{0} \\
& && \text{Tr}(\mathbf{X}) = 1 \\
& && \text{Tr}(\mathbf{\Theta}_{2k}\mathbf{X}) = 0, \quad k = 1, 2, \dots, \frac{M-1}{2} \\
& && \text{rank}(\mathbf{X}) = 1 \\
& && \mathbf{X} \succeq \mathbf{0}
\end{aligned} \tag{1.17}$$

The constraint  $\text{rank}(\mathbf{X}) = 1$  is non-convex, whereas as all the constraints along with the objective function are linear and hence convex in  $\mathbf{X}$ . The Problem 1.17 can be made convex if we drop the unity rank constraint [11]. Here we drop the

unity constraint, hence Problem 1.17 is reduced to,

$$\begin{aligned}
& \underset{\mathbf{X}}{\text{minimize}} && \text{Tr}(\mathbf{R}\mathbf{X}) \\
& \text{subject to} && \mathbf{A}\mathbf{X} = \mathbf{0} \\
& && \text{Tr}(\mathbf{X}) = 1 \\
& && \text{Tr}(\mathbf{\Theta}_{2k}\mathbf{X}) = 0, \quad k = 1, 2, \dots, \frac{M-1}{2} \\
& && \mathbf{X} \succeq 0
\end{aligned} \tag{1.18}$$

Problem 1.18 is solved using CVX toolbox [6], the output of which is the matrix  $\mathbf{X}$ , the analysis filter obtained using the spectral factorization of the autocorrelation function obtained from matrix  $\mathbf{X}$ . Chapter 3 discuss the problem formulation in detail.

Earlier A. Karmakar [9] employed a SDP [27] based approach to design the orthogonal filter banks, in which stop band energy was taken as the optimality criterion. Yan and Lu [30] designed orthogonal filter banks using polynomial optimization techniques. Zhang and Davidson [31] designed signal adapted wavelets using SDP based approach. Dumitrescu and Popeea [3, 4] designed the compaction filters and orthogonal filter banks using the SDP based approach.

## 1.4 Organization of the Report

The report is organized into 5 chapters. Chapter 2 gives the brief overview of the time-frequency uncertainty literature along with the earlier work done to design filters and filter banks based on time-frequency uncertainty. The detailed formulation of all the three proposed design problems has been discussed in Chapter 3. Chapter 4 discusses the results, in which we present eight design examples. Report ends with Chapter 5 providing critical remarks on the proposed framework along with the scope of the future work.

# Chapter 2

## Literature Survey

### 2.1 Time-Frequency Uncertainty

In this section we discuss the time-frequency uncertainty, the fact which tells that a signal cannot be localized in time and frequency simultaneously beyond a certain extent. To understand this principle more closely, take an example of a signal, the frequency of which increases with time, such signals are known as chirps. Consider a linear chirp whose frequency increases linearly with time. If we analyze the signal on time-frequency plane, a smooth linear curve cannot be obtained, the time-frequency plot of the signal would be consisting of small rectangles, which have a certain width in time and frequency, within that box the time-frequency behavior is uncertain, this explains the notion of uncertainty, the question that can be asked is, up to what extent we can reduce the area of the rectangle? In other words, up to what extent the uncertainty can be reduced. This section discusses about the extent of the uncertainty in continuous time as well as in discrete time. We also discuss the connection between the discrete and the continuous time uncertainty in this section.

#### 2.1.1 Uncertainty in Continuous-Time Domain

Gabor's uncertainty principle [5] essentially states:

“A signal cannot be localized simultaneously in time and frequency arbitrarily.”

The above statement is essentially the signal processing version of uncertainty which was given by Gabor. The signal processing version of uncertainty principle [5] is directly associated with the Heisenberg’s uncertainty principle in quantum mechanics. Let  $x(t) \in L^2(\mathbb{R})$  be a even symmetric function with unity norm, i.e,  $\int_{\mathbb{R}} |x(t)|^2 dt = 1$ .

Then according to Gabor’s uncertainty principle [5] :

$$\int_{\mathbb{R}} t^2 |x(t)|^2 dt \frac{1}{2\pi} \int_{\mathbb{R}} \Omega^2 |X(\Omega)|^2 d\Omega \geq \frac{1}{4} \quad (2.1)$$

where  $X(\Omega)$  is the Fourier transform of  $x(t)$ . The above inequality can be written in time domail using Parseval’s theorem as,

$$\int_{\mathbb{R}} t^2 |x(t)|^2 dt \int_{\mathbb{R}} |x'(t)|^2 dt \geq \frac{1}{4} \quad (2.2)$$

From (2.2), we can say that the signal spread in time and the energy in its derivative cannot both be reduced arbitrarily.

Inequality (2.2) implies that the time-frequency product  $\Delta_x = \sigma_t^2 \sigma_\Omega^2$  of a signal  $x(t)$  is bounded below by 0.25, i.e.,

$$\Delta_x = \sigma_t^2 \sigma_\Omega^2 \geq \frac{1}{4} \quad (2.3)$$

where

$$\sigma_t^2 = \int_{\mathbb{R}} t^2 |x(t)|^2 dt$$

and

$$\sigma_\Omega^2 = \frac{1}{2\pi} \int_{\mathbb{R}} \Omega^2 |X(\Omega)|^2 d\omega$$

In (2.3) equality is achieved only for the Gaussian signal.

### 2.1.2 Uncertainty in Discrete-Time Domain

In this subsection, we briefly describe the uncertainty in discrete time domain. Let  $h(n)$  be a real valued, even symmetric discrete-time sequence in  $l^2(\mathbb{Z})$ . The Discrete-Time Fourier Transform (DTFT) of  $h(n)$  is given by,

$$H(\omega) = \sum_{n=-\infty}^{\infty} h(n) e^{-j\omega n} \quad (2.4)$$

and the energy of the sequence  $h(n)$  is given by,

$$E = \sum_{n=-\infty}^{\infty} |h(n)|^2 = \frac{1}{2\pi} \int_{-\pi}^{\pi} |X(w)|^2 d\omega$$

, The integral in above equation is equal to the summation, the same can be deduced by Parseval's theorem. The time variance of the sequence is defined as [7, 8];

$$\sigma_n^2 = \frac{1}{E} \sum_{n=-\infty}^{\infty} n^2 |h(n)|^2 \quad (2.5)$$

The frequency variance for a low-pass sequence  $h(n)$  is defined as [7, 8]

$$\sigma_\omega^2 = \frac{1}{2\pi E} \int_{-\pi}^{\pi} \omega^2 |H(\omega)|^2 d\omega \quad (2.6)$$

The time-frequency product

$$\Delta_h = \sigma_n^2 \sigma_\omega^2 \geq \frac{(1 - |H(\pi)|)^2}{4} \quad (2.7)$$

is also lower bounded [7].  $\sigma_n^2 \sigma_\omega^2 = 0$  for the sequences with  $H(\pi) = 1$ , here the question arises, "Are the sequences with  $H(\pi) = 1$  have no uncertainty?" Of-course the answer to this question is no, that's the reason the uncertainty given by [7] is best suited for low-pass sequences.

There are several other notions of time-frequency localization and the corresponding discrete time uncertainty that have been taken into account [1, 2, 7, 8,

17, 20, 25]. E. Breitenberger [1] argued that the discrete frequency variance stated in [7, 8] changes if we shift the DTFT of the sequence, whereas the variance of a function must be invariant to the translation. E. Breitenberger [1] presented a circular moment based definition of frequency variance which is invariant of shifting.

Discrete time signals are obtained after sampling a continuous time signal. It is well known that a bandlimited continuous time signal can be reconstructed from its samples if the sampling is done over the Nyquist rate. Venkatesh et al. [28] reported the time-frequency localization of the bandlimited signals. It was verified in the work by Venkatesh et al. [28] that for bandlimited signals the lower bound on the time-frequency product can be very closely achieved. Any discrete sequence with at least one zero at  $z = -1$  can be considered as a sampled version of a continuous time signal. Hence we can say that time-frequency localization of the sequences with zeros at  $z = -1$  directly resembles with the time-frequency localization of the corresponding continuous time signal. The same fact encourages us to take the time-frequency measures of the low-pass sequences (with zeros at  $z = -1$ ) as the optimality criterion.

## **2.2 Earlier Work on Time Frequency Localizarion Based Filters and Filter Banks**

L. Shen and Z. Shen [19] verified the effectiveness of the time-frequency localization based filter banks on compression of the images. They used zero tree algorithm, in which decomposition of the image was done by time localized filter bank and the frequency localization based filter banks. Decomposition of image on larger scales was done by frequency localized filter banks, whereas at low-levels the decomposition was done by time-localized filter banks. It was shown that the scheme keeps more texture details of the original images.

M. Sharma et al. [18] devised a framework to design time-frequency localized

biorthogonal filter banks. Convex combination of time and frequency variance (CCTFV) was taken as the objective function in the work. The objective function was formulated in convex quadratic form, whereas the constraints were formulated in linear form. Eigenfilter based approach was used to solve the convex problem. In one of the design problem proposed, we used the same objective function to design the orthogonal filter bank.

D. Tay [23, 24] designed a class of linear phase biorthogonal half-band pair filter banks. Balanced-uncertainty metric proposed by D. Monro and B. G. Sherlock [12] was taken as an optimality criterion. This metric is the weighted summation of time variance and frequency variance of the filter to be designed.

R. Parhizkar et al. [16] devised a methodology to generate the sequences with minimum time-frequency spread. Semidefinite programming was used to design the sequence. The time variance of the sequence was minimized for a given frequency variance. The Design Problem 2 and 3 of the present work are inspired by the approach used in [16].

J. Morris et al. [13–15] designed discrete time wavelets taking the time-frequency localization as an optimal criterion. In [13] minimum time duration wavelets were designed using a technique called adaptive stimulated annealing. In [14] a framework was proposed to design optimum bandwidth wavelets using the same technique. Whereas in [15] the product of the time duration and the bandwidth was taken as an optimality criterion to design time-frequency localized wavelets. However vanishing moments constraints were not taken into the account.

## Chapter 3

### The Devised Framework

Filter bank designing is basically an optimization problem in which an objective function is to be minimized (or maximized) satisfying the constraints being imposed. The two primary constraints for designing the orthogonal filter banks are the vanishing moment (VM) constraint and the double shift orthogonality (DSO) constraints. The third constraint that is been imposed in the present designs is the unity norm constraint, i.e. the norm of the filter impulse response should be unity. The aim is to design the time-frequency localization optimized orthogonal filter bank. In the present work, three design problems have been formulated and solved to design the optimal filter banks. All the three constraints are common to the three design problems. All the three design problems have been solved using iterative semidefinite programming as explained in Section 3.7.

In the Design Problem 1, the objective function is taken to be the convex combination of time variance and frequency variance of the analysis low-pass filter (CCTFV). The objective function is given as;

$$\Phi = \alpha\sigma_n^2 + (1 - \alpha)\sigma_\omega^2 \quad (3.1)$$

Where  $\alpha \in [0, 1]$  and  $\sigma_n^2$  and  $\sigma_\omega^2$  is the time variance and the frequency variance of the filter impulse response, respectively. Time variance and frequency variance are



described and formulated in the Sections 3.1 and 3.2 respectively. The CCTFV is formulated in the Section 3.3. The problem is to find a vector (i.e. the filter impulse response) that minimizes  $\Phi$  subjected to the three constraints. Iterative semidefinite programming has been used to solve the problem. The detailed description and formulation of the objective function and constraints is described in this chapter.

In the Design Problem 2, the frequency variance is fixed to a constant value and then the time variance is minimized. Hence the objective function taken in this approach is the time variance itself, where as one constraint has been increased, that constraint is the fixed frequency variance. The whole approach is described in detail in sub-section 3.8.2.

In the Design Problem 3, the frequency variance is minimized after fixing the time variance to a constant value. The objective function is the frequency variance itself with one more constraint along with the three constraints, i.e. the fixed time variance. Sub-section 3.8.2 describes the third approach.

## 3.1 Time Variance

Consider a causal FIR filter with the following difference equation.

$$y(n) = \sum_{k=0}^M h(k)x(n-k) \quad (3.2)$$

Where  $M \in \mathbb{N}$  and  $x(n)$  is the input to the filter and  $y(n)$  is the output of the filter. Length of the filter is  $M + 1$ . Time variance of a discrete time signal is a measure of the spread of a signal in the time domain. Time variance of a unity norm sequence  $h(n)$  is given by

$$\sigma_n^2 = \sum_{n=-\infty}^{\infty} (n - n_0)^2 |h(n)|^2 \quad (3.3)$$

Where  $n_0$  is the time center and is given by

$$n_0 = \sum_{n=-\infty}^{\infty} n|h(n)|^2 \quad (3.4)$$

In the present case

$$h(n) = 0, \forall n \in \{(n < 0) \cup (n > M)\}$$

Hence equation 3.3 can be written as

$$\sigma_n^2 = \sum_{n=0}^M (n - n_0)^2 |h(n)|^2 \quad (3.5)$$

where

$$n_0 = \sum_{n=0}^M n|h(n)|^2 \quad (3.6)$$

Equation 3.5 can be written in matrix form as follows,

$$\sigma_n^2 = \mathbf{h}^T \mathbf{P} \mathbf{h} \quad (3.7)$$

where  $\mathbf{h} \in \mathbb{R}^{M+1}$  is given in equation 3.14 and  $\mathbf{P} \in \mathbb{R}^{(M+1) \times (M+1)}$  and is given by,

$$\mathbf{P} = \begin{bmatrix} (0 - n_0)^2 & & & & \\ & (1 - n_0)^2 & & & 0 \\ & & (2 - n_0)^2 & & \\ & & & \ddots & \\ 0 & & & & (M - n_0)^2 \end{bmatrix} \quad (3.8)$$

Hence the  $(k, l)^{th}$  element of the matrix  $\mathbf{P}$  is obtained as

$$\mathbf{P} = \begin{cases} (k - n_0)^2 & \text{if } k = l \\ 0 & \text{if } k \neq l \end{cases} \quad (3.9)$$

Where  $k, l \in \{0, 1, 2, \dots, M\}$ . Note that the matrix  $\mathbf{P}$  is a real symmetric positive definite matrix, as  $\mathbf{P}$  is diagonal matrix with positive diagonal elements. The Equation 3.7 can also be written in the following form,

$$\begin{aligned} \sigma_n^2 &= \text{Tr}(\sigma_n^2) \quad (\because \text{a scalar is equal to its trace}) \\ \implies \sigma_n^2 &= \text{Tr}(\mathbf{h}^T \mathbf{P} \mathbf{h}) \quad (\text{Using Eq. 3.7}) \\ \implies \sigma_n^2 &= \text{Tr}(\mathbf{P} \mathbf{h} \mathbf{h}^T) \quad (\because \text{Tr}(\mathbf{ABC}) = \text{Tr}(\mathbf{BCA})) \end{aligned}$$

Where  $\mathbf{A}, \mathbf{B}$  and  $\mathbf{C}$  are the matrices of relevant sizes.

$$\text{Let } \mathbf{X} = \mathbf{h} \mathbf{h}^T$$

Hence

$$\sigma_n^2 = \text{Tr}(\mathbf{P} \mathbf{X}) \quad (3.10)$$

## 3.2 Frequency Variance

Frequency variance of a sequence  $h(n)$  is a measure of the spread of the spectrum of the signal. The spectrum could be the DTFT of the sequence or the DFT of the sequence. In the present work, variance of the DTFT of the sequence has been taken into account and variance of the DTFT of the signal has been called frequency variance in the whole report. The frequency variance of a real valued unity norm discrete time sequence  $h(n)$  is given by

$$\sigma_\omega^2 = \int_0^\pi \omega^2 |H(\omega)|^2 \frac{d\omega}{\pi} \quad (3.11)$$

Where,  $H(\omega)$  is the DTFT of  $h(n)$ .

To formulate the frequency variance in the matrix form, it is necessary to formulate the DTFT first. The Discrete Time Fourier Transform (DTFT) of the  $h(n)$  is given by

$$H(\omega) = \sum_{n=0}^M h(n)e^{-j\omega n} \quad (3.12)$$

where  $\omega$  is the normalized digital frequency. Equation 3.12 can be written in the following form.

$$H(\omega) = \mathbf{e}^T(\omega)\mathbf{h} = \mathbf{h}^T\mathbf{e}(\omega) \quad (3.13)$$

where

$$\mathbf{h} = \begin{bmatrix} h(0) & h(1) & \dots & h(M-1) & h(M) \end{bmatrix}^T, M \in \mathbb{N} \quad (3.14)$$

and

$$\mathbf{e}(\omega) = \begin{bmatrix} e^{-j0\omega} & e^{-j1\omega} & e^{-j2\omega} & \dots & \dots & e^{-jM\omega} \end{bmatrix}^T, \omega \in [-\pi, \pi] \quad (3.15)$$

Now

$$\begin{aligned} |H(\omega)|^2 &= H(\omega)H^*(\omega) \\ &= \mathbf{h}^T\mathbf{e}(\omega)\{\mathbf{h}^T\mathbf{e}(\omega)\}^H \\ &= \mathbf{h}^T\mathbf{e}(\omega)\mathbf{e}^H(\omega)\mathbf{h} \end{aligned} \quad (3.16)$$

Substituting the result obtained from Equation 3.16 in Equation 3.11 following expression is obtained for the frequency variance.

$$\sigma_\omega^2 = \mathbf{h}^T \left\{ \int_0^\pi \omega^2 \mathbf{e}(\omega)\mathbf{e}^H(\omega) \frac{d\omega}{\pi} \right\} \mathbf{h} \quad (3.17)$$

Eq. 3.17 can be expressed as;

$$\sigma_\omega^2 = \mathbf{h}^T \mathbf{F} \mathbf{h} \quad (3.18)$$

Where  $\mathbf{F} \in \mathbb{C}^{(M+1) \times (M+1)}$  and the  $\{(k, l)^{\text{th}}\}$  element of the frequency variance matrix  $\mathbf{F}$  can be obtained as;

$$\mathbf{F}_{k,l} = \begin{cases} \frac{\pi^2}{3} & \text{if } k = l \\ \frac{\pi^2(-1)^{(l-k)}}{j(l-k)} + \frac{2\pi(-1)^{(l-k)}}{(l-k)^2} + \frac{2(1-(-1)^{(l-k)})}{j(l-k)^3} & \text{if } k \neq l \end{cases} \quad (3.19)$$

Where  $k, l \in \{0, 1, 2, \dots, M\}$ . Note that the matrix  $\mathbf{F}$  is a complex hermitian symmetric positive definite matrix. The derivation for frequency variance matrix is given in the Appendix A.1. Eq. 3.18 can be written in trace form as,

$$\begin{aligned} \sigma_\omega^2 &= \text{Tr}(\mathbf{F}\mathbf{h}\mathbf{h}^T) \\ &= \text{Tr}(\mathbf{F}\mathbf{X}) \end{aligned} \quad (3.20)$$

### 3.3 The CCTFV

CCTFV is the convex combination of time variance and frequency variance. Eq. 3.1 describes CCTFV mathematically. Substituting the value of  $\sigma_n^2$  and  $\sigma_\omega^2$  from Eq. 3.7 and Eq. 3.18 in Eq. 3.1, we get

$$\begin{aligned} \Phi &= \alpha \mathbf{h}^T \mathbf{P} \mathbf{h} + (1 - \alpha) \mathbf{h}^T \mathbf{F} \mathbf{h} \\ \text{i.e. } \Phi &= \mathbf{h}^T \{ \alpha \mathbf{P} + (1 - \alpha) \mathbf{F} \} \mathbf{h} \end{aligned}$$

Where,  $\alpha \in [0, 1]$

Hence,

$$\Phi = \mathbf{h}^T \mathbf{R} \mathbf{h} \quad (3.21)$$

Where

$$\mathbf{R} = \alpha \mathbf{P} + (1 - \alpha) \mathbf{F} \quad (3.22)$$

Equation 3.1 can be written as

$$\begin{aligned}\Phi &= \text{Tr}(\mathbf{R}\mathbf{h}\mathbf{h}^T) \\ &= \text{Tr}(\mathbf{R}\mathbf{X})\end{aligned}\tag{3.23}$$

### 3.4 The Double Shift Orthogonality

To design a perfect reconstruction filter bank, impulse response of the analysis low-pass filter must be orthogonal to its even shifts i.e. the dot product of the sequence to its even shifts must be zero. In other words the autocorrelation function  $r_h(k)$  of the filter impulse response  $h(n)$  must be zero at even value of  $k$  except  $k = 0$ . To formulate DSO constraints, it is necessary to understand the formulation of autocorrelation function. ACF of a finite length sequence can be formulated in quadratic form [4] and hence in SDP form using trace parameterization. Next sub-section describes the formulation of ACF.

#### 3.4.1 Formulation of ACF

Autocorrelation function of a finite length sequence is a symmetric odd length sequence. As ACF is symmetric, only right half part can be computed, the remaining coefficients can be computed employing symmetry. Filter impulse response  $h(n)$  is non-zero over the range  $n = 0$  to  $n = M$ , where  $M$  is an odd natural number. Mathematically

$$h(n) = 0, \forall n \in \{(n < 0) \cup (n > M)\}$$

It can be noted that, the ACF,  $r_h(k)$  of  $h(n)$  is non-zero over the range  $k = -M$  to  $k = M$ , mathematically

$$r_h(k) = 0, \forall |k| > M$$

Also,

$$r_h(k) = r_h(-k)$$

Therefore, all the information of ACF is contained in the coefficients from  $k = 0$  to  $k = M$ , which is given by the following equation.

$$\begin{aligned} r(k) &= \sum_{n=k}^M h(n)h(n-k) \\ &= \mathbf{h}^T \mathbf{Q}_k \mathbf{h}, \quad k = \{0, 1, \dots, M\} \end{aligned} \quad (3.24)$$

Where  $Q_0 = I_{M+1}$  is the identity matrix of order  $M + 1$  and

$$Q_k = \frac{1}{2} \text{Toep}(e_k), \quad k \neq 0 \quad (3.25)$$

and

$$e_k = [\underbrace{0 \ 0 \ 0 \ \dots \ 0}_{k \text{ zeros}} \ 1 \ 0 \ \dots \ 0]^T \quad (3.26)$$

note that,  $e_k \in \mathbb{R}^{M+1}$ .

For Example, for  $M = 3$

$$\begin{aligned} e_1 &= \begin{bmatrix} 0 & 1 & 0 & 0 \end{bmatrix} \\ 2Q_1 &= \begin{bmatrix} 0 & 1 & 0 & 0 \\ 1 & 0 & 1 & 0 \\ 0 & 1 & 0 & 1 \\ 0 & 0 & 1 & 0 \end{bmatrix} \end{aligned}$$

and

$$\begin{aligned} e_2 &= \begin{bmatrix} 0 & 0 & 1 & 0 \end{bmatrix} \\ 2Q_2 &= \begin{bmatrix} 0 & 0 & 1 & 0 \\ 0 & 0 & 0 & 1 \\ 1 & 0 & 0 & 0 \\ 0 & 1 & 0 & 0 \end{bmatrix} \end{aligned}$$

Hence for each index  $k$  there is a quadratic form  $\mathbf{h}^T \mathbf{Q}_k \mathbf{h}$ . In SDP form ACF can be written as follows,

$$r_h(k) = \text{Tr}(\mathbf{Q}_k \mathbf{X}) \quad (3.27)$$

Following equation describes the DSO constraint,

$$r_h(2k) = 0 \quad k = 1, 2, \dots, \frac{M-1}{2} \quad (3.28)$$

Eq. 3.28 in SDP form as,

$$\text{Tr}(Q_{2k} X) = 0 \quad k = 1, 2, \dots, \frac{M-1}{2} \quad (3.29)$$

The above form is important because it can be directly put in the semidefinite program.

## 3.5 Vanishing Moments

In certain applications, especially in the design of wavelet filter banks, the low-pass filter is required to be regular. A low-pass filter  $H(z)$  is said to be  $V$ -regular if it has  $V$  multiple zeros at  $z = -1$ , or equivalently, the frequency response of the filter satisfies;

$$\left. \frac{d^k H(e^{j\omega})}{d\omega^k} \right|_{\omega=\pi} = 0, \quad k = 0, 1, 2, \dots, V-1 \quad (3.30)$$

If  $H(z)$  has a zero of multiplicity  $V$  at  $z = -1$ , then the wavelet constructed from two-channel filter banks shall have  $V$  consecutive vanishing moments, mathematically,

$$\int_{\mathbb{R}} t^k \psi(t) dt = 0, \quad k = 0, 1, \dots, V-1 \quad (3.31)$$



The vanishing moment constraint has been formulated in the time domain. For  $k = 0$ , Eq. 3.30 can be written as,

$$H(e^{j\pi}) = 0$$

Hence

$$\sum_{n=0}^M h(n)(-1)^n = 0 \quad (3.32)$$

Also, for  $k = 1, 2, 3, \dots, V-1$  Eq. 3.30 can be written in time domain as,

$$\sum_{n=0}^M (-1)^n n^k h(n) = 0 \quad k = 1, 2, \dots, V-1 \quad (3.33)$$

Eq. 3.32 and 3.33 can collectively written as,

$$\mathbf{A}\mathbf{h} = \mathbf{0} \quad (3.34)$$

Where

$$\mathbf{A} \in \mathbb{R}^{V \times (M+1)}$$

and the expression for computing the elements of matrix  $\mathbf{A}$  is given as follows;

$$A_{k,l} = \begin{cases} (-1)^l & \text{if } k = 0 \\ l^k (-1)^l & \text{if } k \neq 0 \end{cases} \quad (3.35)$$

Where,  $k \in \{0, 1, 2, \dots, V-1\}$  and  $l \in \{0, 1, 2, \dots, M\}$ . As an example, the matrix  $\mathbf{A}$  for  $V = 3$  and  $M = 5$  is given as;

$$A = \begin{bmatrix} 1 & -1 & 1 & -1 & 1 & -1 \\ 0 & -1 & 2 & -3 & 4 & -5 \\ 0 & -1 & 4 & -9 & 16 & -25 \end{bmatrix} \quad (3.36)$$

Post multiplying Eq. 3.34 by  $\mathbf{h}^T$ , we get

$$\mathbf{A}\mathbf{h}\mathbf{h}^T = \mathbf{0}$$

As  $\mathbf{X} = \mathbf{h}\mathbf{h}^T$ , The above equation can be written as,

$$\mathbf{A}\mathbf{X} = \mathbf{0} \quad (3.37)$$

This completes the formulation of vanishing moment constraint.

## 3.6 Filter Norm

The  $l^2$  norm of the impulse response,  $h(n)$  of analysis low-pass filter is desired to be unity, mathematically

$$\|\mathbf{h}\|_2 = \sqrt{\sum_{n=-\infty}^{\infty} |h(n)|^2} = 1 \quad (3.38)$$

The above equation can be re-written as follows,

$$\begin{aligned} \|\mathbf{h}\|_2 &= \mathbf{h}^T \mathbf{h} \\ &= \text{Tr}(\mathbf{h}\mathbf{h}^T) = 1 \end{aligned} \quad (3.39)$$

The unity norm constraint has been imposed in all the three approaches. The reason for this constraint is the definition of frequency variance (Eq. 3.11), which has been used in the present work. Equation 3.11 is valid definition of variance if and only if norm of  $h(n)$  is unity. As,  $h(n) \in l^2(\mathbb{Z})$  Also by Parseval's theorem,

$$\sum_{n=-\infty}^{\infty} |h(n)|^2 = \frac{1}{2\pi} \int_{-\pi}^{\pi} |H(e^{-j\omega})|^2 d\omega \quad (3.40)$$

Hence,

$$\frac{1}{2\pi} \int_{-\pi}^{\pi} |H(e^{-j\omega})|^2 d\omega = \frac{1}{\pi} \int_0^{\pi} |H(e^{-j\omega})|^2 d\omega = 1 \quad (3.41)$$

As  $|H(e^{-j\omega})|^2$  is positive for all values of  $\omega$  and the area under  $\frac{|H(e^{-j\omega})|^2}{2\pi}$  is unity,  $\frac{|H(e^{-j\omega})|^2}{2\pi}$  can be considered as a density function. This validates the frequency variance definition described in Eq. 3.11. Hence unity norm constraint is important.

The same constraint also validates the definition of time variance described in Eq. 3.3.

### 3.7 Iterative SDP

The time center of the sequence  $h(n)$  is given by the following equation,

$$n_0 = \sum_{n=0}^M n |h(n)|^2 \quad (3.42)$$

The matrix,  $\mathbf{P}$  associated time variance can be computed if and only if the time center,  $n_0$  of  $h(n)$  is known. On the other hand we want to design the optimal filter  $h(n)$ , which is unknown. Hence we can not compute the matrix  $\mathbf{P}$  given in Eq. 3.8.

This problem is handled by using an iterative SDP approach. At first an arbitrary value of  $n_0 \in [0, M]$  is taken and then the solution for  $h(n)$  is obtained. The obtained  $h(n)$  could have different value of the time center, (say  $n'_0$ ). We want that the value of time center (which was set before solving the problem) to be equal to the time center of the obtained filter impulse response. To achieve the same, we again set the time center to  $n'_0$  and solve the problem to find  $h(n)$ , the time center of the obtained  $h(n)$ , (say  $n''_0$ ) would appear close to  $n'_0$ . It has been noticed that the time center of the obtained filter tries to follow the time center which was set before solving the problem, it happens after first iteration. In the

present work we have used up to three iterations. The proof of the fact is yet to derived.

## 3.8 The Design Problems

This section explains the three design problems that has been formulated and solved, to design the time-frequency localization optimized orthogonal wavelet filter banks. All the three design problems are solved using the iterative semidefinite programming explained in Sec. 3.7. The output of the optimizaion technique used is the matrix  $\mathbf{X}^{\text{opt}}$ . The filter vector  $\mathbf{h}$  given in Eq. 3.14, is to be calculated from the optimal matrix  $\mathbf{X}^{\text{opt}}$ . To calculate  $\mathbf{h}$ , the auto correlation function is first calculated using the relation given below.

$$\begin{aligned} r_h(0) &= 1 \\ r_h(k) &= \text{Tr}(\mathbf{Q}_k \mathbf{X}^{\text{opt}}), \quad k = 1, 2, \dots, M; \end{aligned} \tag{3.43}$$

As ACF is a symmetric sequence, the positive half from  $k = 0$  to  $k = M$ , of the ACF has been calculated, the negative half from  $k = -M$  to  $k = -1$  can be calculated employing the symmetry ( $r_h(-k) = r_h(k)$ ). After computing the ACF, the filter impulse response is computed using spectral factorization. The minimum phase spectral factor is taken into the account in the present work.

In all the three design problem, an objective function is minimized subjected to three or four kinds of constraints. All the three design problems are convex in  $\mathbf{X}$  as explained in Section 1.3 of Chapter 1. The double shift orthogonality, the vanishing moment and the unity norm constraints(explained in Setion 3.4, 3.5 and 3.6) are common in all the three problems.

### 3.8.1 The Design Problem 1

In the Design Problem 1, the CCTFV (explained in Sec. 3.3) is taken as an objective function, which is to be minimized subjected to the three constraints.

The problem to be solved is given below,

$$\begin{aligned}
& \underset{\mathbf{X}}{\text{minimize}} \quad \text{Tr}(\mathbf{R}\mathbf{X}) \quad (\text{refer Eq.3.23 in Sec. 3.3}) \\
& \text{subject to} \\
& \quad \text{Tr}(\mathbf{Q}_{2k}\mathbf{X}) = 0, \quad k = 1, 2, \dots, \frac{M-1}{2} \quad (\text{refer Eq. 3.29 in Sec. 3.4}) \quad (3.44) \\
& \quad \mathbf{A}\mathbf{X} = \mathbf{0} \quad (\text{refer Eq. 3.37 in Sec. 3.5}) \\
& \quad \text{Tr}(\mathbf{X}) = 1 \quad (\text{refer Eq. 3.39 in Sec. 3.6})
\end{aligned}$$

The minimization is subjected to the three constraints, namely the double shift orthogonality, the vanishing moment and the unity norm constraint. Formulation for all the three constraints, i.e. DSO, VM and the unity norm constraint, are explained in Sec. 3.4, 3.5 and 3.6 respectively. The problem is solved employing iterative SDP as explained in Sec. 3.7. After solving the problem using iterative SDP, the optimal matrix  $\mathbf{X}^{\text{opt}}$ , satisfying all the constraints, is obtained. Now the filter coefficients need to be computed from the optimal matrix  $\mathbf{X}^{\text{opt}}$ . To find the filter coefficients, at first the autocorrelation function is computed followed by the computation of the filter coefficients using spectral factorization of ACF.

### 3.8.2 The Design Problem 2

In the Design Problem 2, the time variance is the objective function, which is to be minimized, after keeping the frequency variance to a fixed value. Hence the design has one more constraint which is the fixed frequency variance. This approach can be beautifully employed if the frequency variance for the particular application is

already known. The design problem can be mathematically expressed as follows,

$$\begin{aligned}
& \underset{\mathbf{X}}{\text{minimize}} \quad \text{Tr}(\mathbf{P}\mathbf{X}) \quad (\text{refer Eq. 3.10 in Sec. 3.1}) \\
& \text{subject to} \\
& \quad \text{Tr}(\mathbf{Q}_{2k}\mathbf{X}) = 0, \quad k = 1, 2, \dots, \frac{M-1}{2} \quad (\text{refer Eq. 3.29 in Sec. 3.4}) \\
& \quad \mathbf{A}\mathbf{X} = \mathbf{0} \quad (\text{refer Eq. 3.37 in Sec. 3.5}) \\
& \quad \text{Tr}(\mathbf{X}) = 1 \quad (\text{refer Eq. 3.39 in Sec. 3.6}) \\
& \quad \text{Tr}(\mathbf{F}\mathbf{X}) = f_0 \quad (\text{refer Eq. 3.20 in Sec. 3.2})
\end{aligned} \tag{3.45}$$

### 3.8.3 The Design Problem 3

In the Design Problem 3, the opposite of the design 2 is done, i.e. the frequency variance is taken as the objective function, which is to be minimized, after keeping the time variance to a fixed value. Mathematically,

$$\begin{aligned}
& \underset{\mathbf{X}}{\text{minimize}} \quad \text{Tr}(\mathbf{F}\mathbf{X}) \quad (\text{refer Eq. 3.20 in Sec. 3.2}) \\
& \text{subject to} \\
& \quad \text{Tr}(\mathbf{Q}_{2k}\mathbf{X}) = 0, \quad k = 1, 2, \dots, \frac{M-1}{2} \quad (\text{refer Eq. 3.29 in Sec. 3.4}) \\
& \quad \mathbf{A}\mathbf{X} = \mathbf{0} \quad (\text{refer Eq. 3.37 in Sec. 3.5}) \\
& \quad \text{Tr}(\mathbf{X}) = 1 \quad (\text{refer Eq. 3.39 in Sec. 3.6}) \\
& \quad \text{Tr}(\mathbf{P}\mathbf{X}) = t_0 \quad (\text{refer Eq. 3.10 in Sec. 3.1})
\end{aligned} \tag{3.46}$$

This approach can be fruitful in the applications, where the required time variance is already known.

The lower bound on the time-frequency product is very well known, which is the global minimum that can be achieved with no constraints. In the present problem the value of the lower bound would be different because of the constraints imposed. The lower bound on the time-frequency uncertainty measures like time-frequency product and the CCTFV is the function of the number of constraints,

which is yet to be derived. In the present design problem, the minimum value of the frequency variance that can be achieved with the constraints imposed is the function of the time variance which is fixed before solving the problem, sounds like the minimum value of  $\sigma_\omega^2$  would be inversely proportional to the fixed value of time variance, but the same could be much more complicated due to the constraints imposed. The exact expression for the minimum value of  $\sigma_\omega^2$  under the constraints is yet to be derived.

### 3.8.4 Constraints on Design Parameters

At first the length of the filter is fixed.  $M$  is the order of the filter, which is an odd natural number. The length of the filter is given by  $L = M + 1$ , which is even, as odd length orthogonal filter bank is fundamentally not possible. Moreover a linear phase orthogonal filter bank is also not possible, which is fundamentally correct, hence symmetric orthogonal filter bank is not possible.

For a given filter length, a limited number of vanishing moments,  $V$  can be achieved. Any arbitrary number of vanishing moments can not be achieved because of the limited degrees of freedom. The number of degrees of freedom equals the Filter Length,  $L$ . Filter length is the only resource to get the desired number of VMs. It has been found empirically that half of the coefficients is the expenditure to satisfy the double shift ortho-normality constraints. The remaining half coefficients can be used for minimization of the objective function and to meet the desired number of vanishing moment. It is obvious that the maximum number of vanishing moments that can be achieved is equal to  $\frac{L}{2}$ , whereas it is not recommended to set  $V = \frac{L}{2}$  because there would be no degree of freedom left which can be used to minimize the objective function.

$$V \leq \frac{L}{2} \quad (3.47)$$

### 3.9 Construction of Wavelets

After obtaining the analysis low-pass filter  $h_0(n) = h(n)$ , the high-pass filter impulse response,  $h_1(n)$  can be obtained using the following relation,

$$h_1(n) = (-1)^n h_0(M - n) \quad (3.48)$$

Where  $M$  is the order of the filters of the underlying filter bank. The members of the synthesis filter bank can be found using the conjugate quadrature symmetry. Wavelets from the filters of the filter banks can be constructed using the cascade algorithm given by M. Vetterli [29]. However, all PR two-channel orthogonal filter banks cannot yield regular wavelet, the necessary and sufficient condition given by G. Strang [22] has been used in the present work. This condition essentially states that the wavelet  $\psi(t)$  and the scaling function  $\phi(t)$  converge into  $L^2(\mathbb{R})$  if and only if the absolute values of all eigenvalues of the transition matrix  $T$ , which is defined below, are less than 1 (except for the simple eigenvalue 1). The Transition matrix is defined as :  $T = (\downarrow 2) \mathbf{2} \mathbf{H} \mathbf{H}^T$ , where  $(\downarrow 2)$  denotes downsampling-by-2 of rows. The  $(k, l)^{th}$  element of the Toeplitz matrix  $\mathbf{H}$  is given as  $[\mathbf{H}]_{k,l} = h_0(k - l)$ ,  $h_0(n)$  are the filter coefficients of the low-pass filter of the underlying orthogonal filter bank, normalized to  $\sum_n h_0(n) = 1$ .

### 3.10 Design Flow

This section describes the flow of the design, to get an optimal time frequency localization optimized orthogonal wavelet filter bank. At first the suitable initial values of the design parameters;  $V \in \mathbb{N}$ ,  $M \in \mathbb{N}$  and  $n_0 \in [0, M]$  is fixed, after keeping the constraints on the value of the design parameters into the account (refer 3.8.4).  $\alpha \in [0, 1]$  is the parameter used in the design problem 1 (3.8.1), whereas  $f_0 \in \mathbb{R}^+$  must be fixed if solving the design problem 2 (3.8.2) and  $t_0 \in \mathbb{R}^+$  must be fixed if solving the design problem 3 (3.8.3).



After selecting the appropriate values of the design parameters, compute the matrices  $\mathbf{P}, \mathbf{F}, \mathbf{A}, \mathbf{Q}_{2k}$  (for  $k = 1, 2, \dots, \frac{M-1}{2}$ ) and  $\mathbf{R}$  using equations 3.8, 3.19, 3.35, 3.25 and 3.22 respectively. Now solve the underlying design problem, formulated in Sec. 3.8 using the iterative SDP approach explained in 3.7, employing CVX toolbox. If SDP solver problem solves the feasible problem, compute the ACF using 3.43 followed by the computation of minimum phase filter  $h_0(n)$  using spectral factorization. Once  $h_0(n)$  is obtained, impulse response of the remaining members of the filter bank (i.e.  $h_1(n)$ ,  $f_0(n)$  and  $f_1(n)$ ) can be computed using conjugate quadrature symmetry.

After obtaining the filter bank wavelet function  $\psi(t) \in L^2(\mathbb{R})$  and scaling function  $\phi(t) \in L^2(\mathbb{R})$  needs to be constructed using cascade algorithm. To ensure the existence of the  $\phi(t)$  and  $\psi(t)$ , the eigenvalues of the transition matrix  $T$  need to be checked as explained in Section 3.9. If the convergence condition is met, construction of wavelets and scaling function can be done using cascade algorithm and hence the valid wavelet orthogonal filter bank can be obtained. If the convergence condition is not met, the perfect reconstruction orthogonal filter bank is obtained, but the same is not a valid wavelet filter bank. The flow chart to design the optimal filter bank is shown in the Fig. 3.1

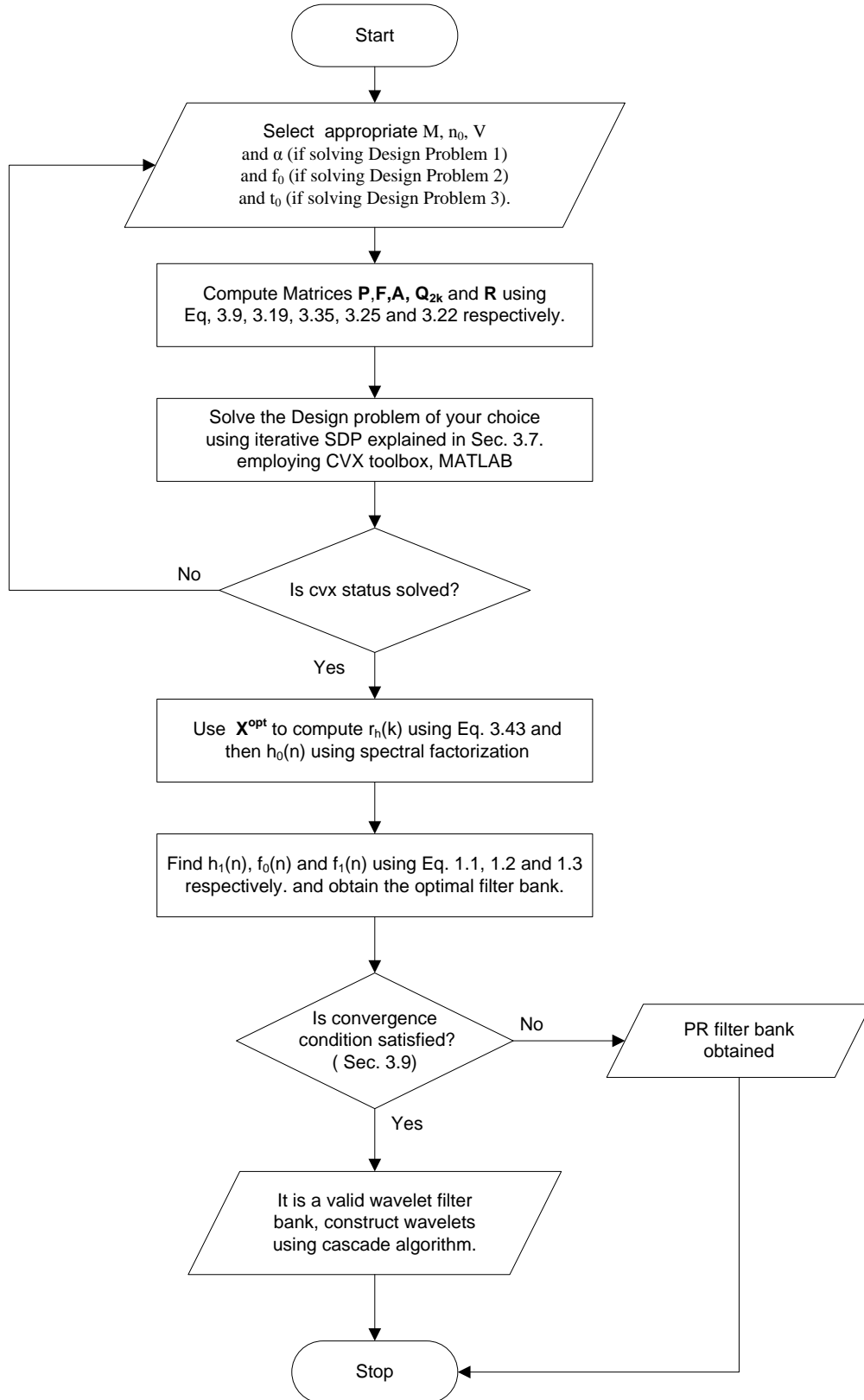


Figure 3.1: Flow chart to design the optimal filter bank

# Chapter 4

## Design Examples

In this chapter, design examples for the three design problems are discussed. We try to show, the effect of number of vanishing moments on the time-frequency properties of the filter banks. The effect of number of vanishing moments on the smoothness of the scaling and the wavelet function can also be clearly seen in the design examples discussed. For the Design Problem 1, the examples are simulated for different values of  $\alpha \in [0, 1]$ . We try to observe the effect of  $\alpha$  on the time-frequency properties of the design examples. We observe that  $\alpha > 0.5$ , affects the smoothness of scaling and wavelet function constructed using cascade algorithm. The discontinuities appear, in the scaling and wavelet function for  $\alpha > 0.5$ , where as the scaling and wavelet function seems smooth for  $\alpha < 0.5$ . Also  $\alpha = 0$  shapes the frequency response of the analysis low-pass filter beautifully as more number of zeros on the unit circle in z-plane but this results in side lobes. It has been observed that the problem solved with  $\alpha = 1$  gives crude frequency response along with less smooth scaling and wavelet functions. Regularity is the measure of smoothness of the scaling and wavelet function. The regularity as a function of  $\alpha$  can be evaluated as a future work.

In the design examples of the Design Problem 2 and 3, we try to get the results achieved in the design examples of Design Problem 1. In Ex. 6, We fixed the value of frequency variance which was achieved in Ex. 2 and we get almost

similar results after designing the filter bank with the same parameters. In Ex. 8, we fix the value of time variance to the value which has been achieved in Ex. 2 and then we solve the design problem with the same parameters as in Ex. 2, again we get similar results. Whereas in Ex. 7, we fixed the value of frequency variance as obtained in Ex. 5 and solved the problem with the same parameters. The comparison between the obtained results is discussed in the Sec. 4.3 of this chapter.

We plot the frequency response,  $H_0(\omega)$  and  $H_1(\omega)$  of the analysis low-pass and high-pass filter. We also plot  $R(\omega)$ , the frequency response of autocorrelation function of the analysis low-pass filter along with  $R(\omega + \pi)$ . The analysis scaling function  $\phi(t)$  and the wavelet function  $\psi(t)$  has been plotted along with the pole-zero plot of the analysis filter.

## 4.1 Design Examples for Design Problem 1

### 4.1.1 Design Example 1

**Parameters Taken:**

$$L = 12$$

$$\alpha = 0.5$$

$$V = 6$$

In this example we try to simultaneously optimize the time and frequency spread by taking  $\alpha = 0.5$ . We have taken  $V = 6$  for the present example, which is the maximum number of vanishing moments that can be achieved for a length 12 orthogonal filter bank. The smooth scaling and the wavelet function are shown in Fig. 4.1c and 4.1d respectively. The  $R(\omega)$  and  $R(\omega + \pi)$ , exhibiting the power complementarity are shown in Fig. 4.1b. The pole-zero plot of analysis low-pass filter is shown in Fig. 4.1e, the six zeros forming the half ring around  $z = -1$ , is

inside the unit circle as the filter is minimum phase.

### 4.1.2 Design Example 2

**Parameters Taken:**

$$L = 12$$

$$\alpha = 0.7$$

$$V = 2$$

In this example, the same design as in Ex. 1 has been solved but with less number of vanishing moments, now we have only 2 vanishing moments instead of 6, also  $\alpha = 0.7$  now. Because of the less number of vanishing moments, the scaling and wavelet function shown in Fig. 4.2c and 4.2d are not as much smooth as that in Ex. 1, the same also affects, the frequency response of the analysis low-pass and high-pass filter as shown in Fig. 4.2a. The response is more crude than that of Ex. 1. The pole-zero plot of the minimum phase analysis low-pass filter is shown in Fig. 4.2e.

### 4.1.3 Design Example 3

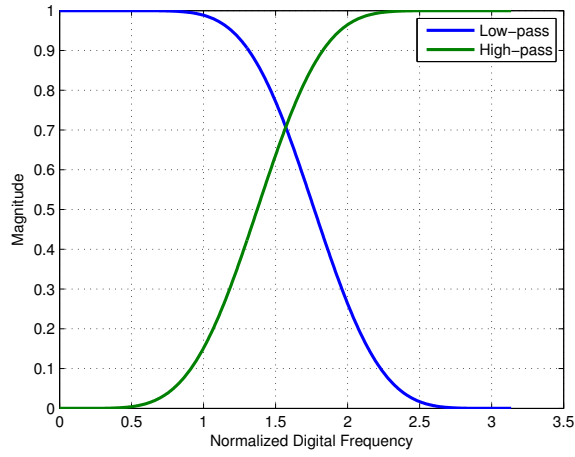
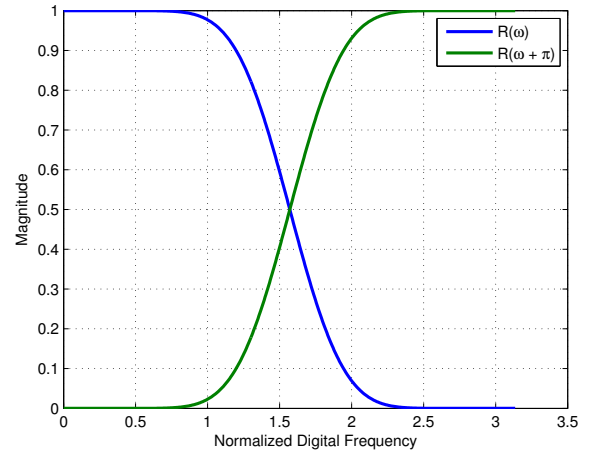
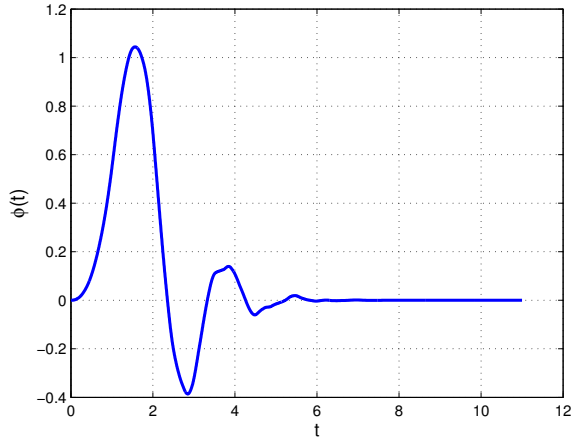
**Parameters Taken:**

$$L = 20$$

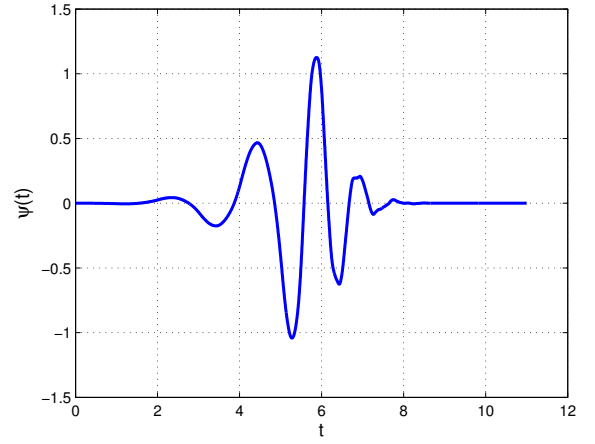
$$\alpha = 0$$

$$V = 6$$

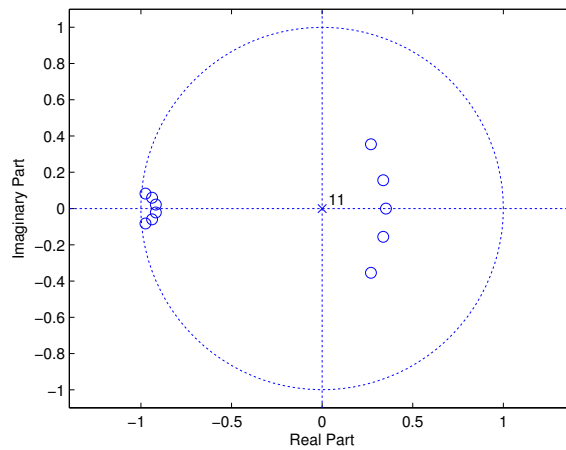
In this example, we try to solve a bigger problem, now the length is 20, with 6 vanishing moments,  $\alpha$  is taken to be 0, i.e. we are only interested in minimizing the frequency variance. Hence we design a purely frequency optimized orthogonal filter bank in this example. Vanishing moments gives the flatness to the frequency

(a) Plot of  $|H_0(\omega)|$  and  $|H_1(\omega)|$  for Example-1(b) Plot of  $R(\omega)$  and  $R(\omega + \pi)$  for Example-1

(c) Analysis Scaling Function for Example-1

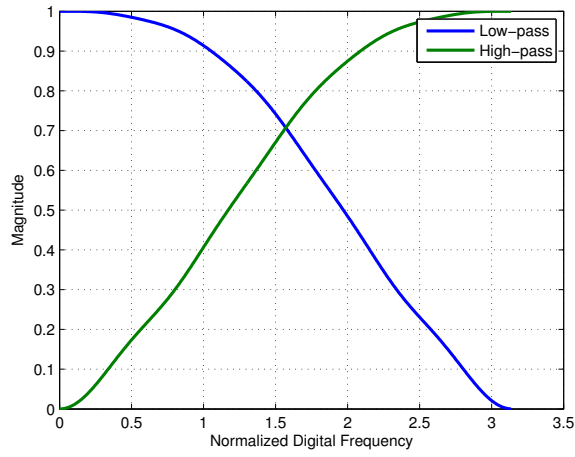
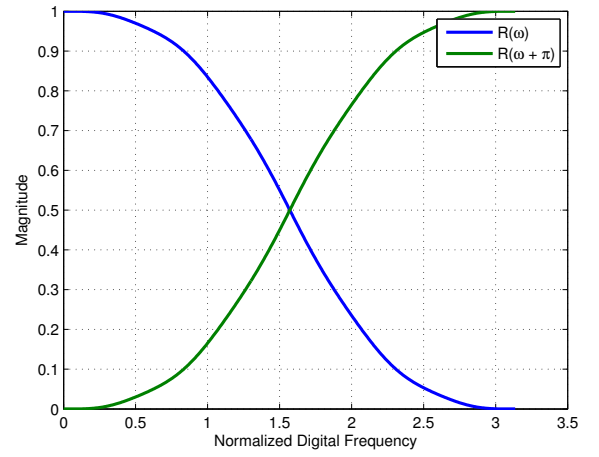
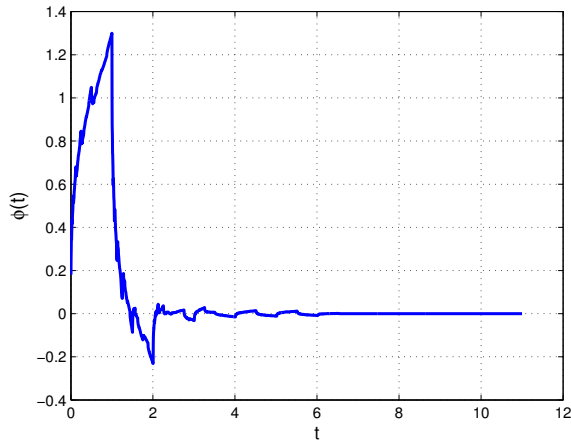


(d) Analysis Wavelet for Example-1

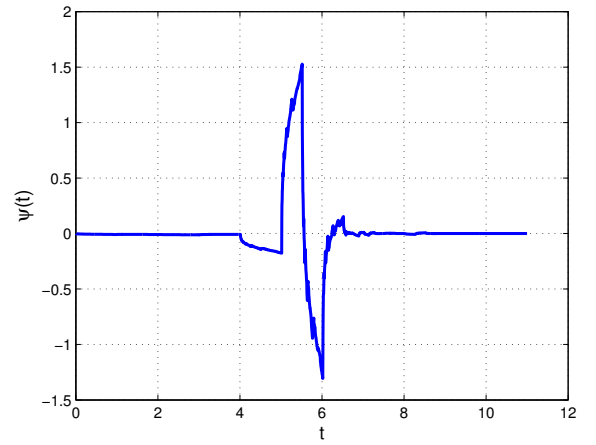


(e) Pole Zero Plot for Example-1

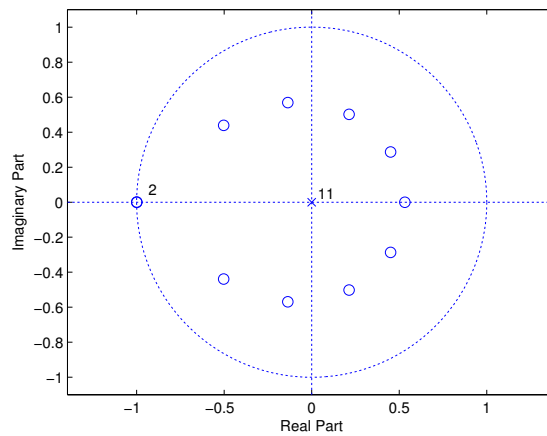
Figure 4.1: Example 1

(a) Plot of  $|H_0(\omega)|$  and  $|H_1(\omega)|$  for Example-2(b) Plot of  $R(\omega)$  and  $R(\omega + \pi)$  for Example-2

(c) Analysis Scaling Function for Example-2



(d) Analysis Wavelet for Example-2



(e) Pole Zero Plot for Example-2

Figure 4.2: Example 2

response at  $\omega = \pi$ , the higher the vanishing moments the better is the flatness, hence we can say vanishing moments help in shaping the frequency response of the filter. In the present example we are trying to minimize the frequency variance only, i.e. we are trying to narrow the filter frequency response as much as possible. Hence we get the narrower response for the present design example as shown in Fig. 4.2a. The remarkable smoothness of the scaling and wavelet function can be seen in Fig. 4.2c and 4.2d respectively. It has been observed that solving the problem with  $\alpha = 0$  gives zeros on the unit circle (other than  $z = -1$ ), the same can be observed in present example in Fig. 4.2e.

#### 4.1.4 Design Example 4

**Parameters Taken:**

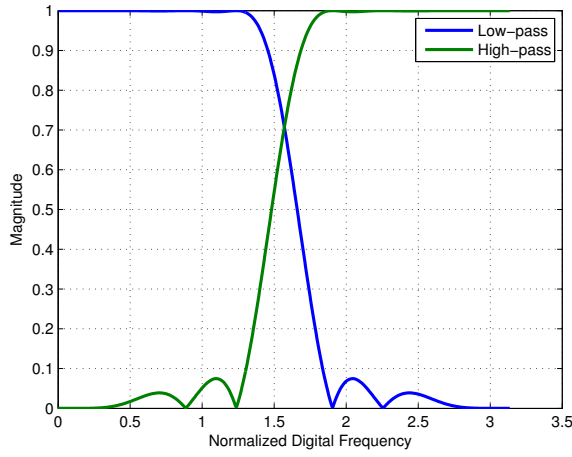
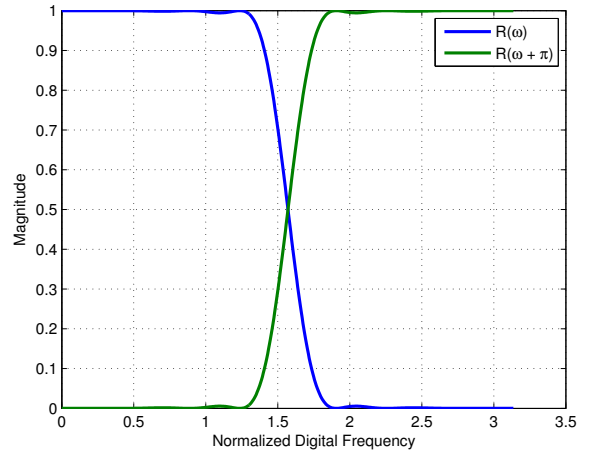
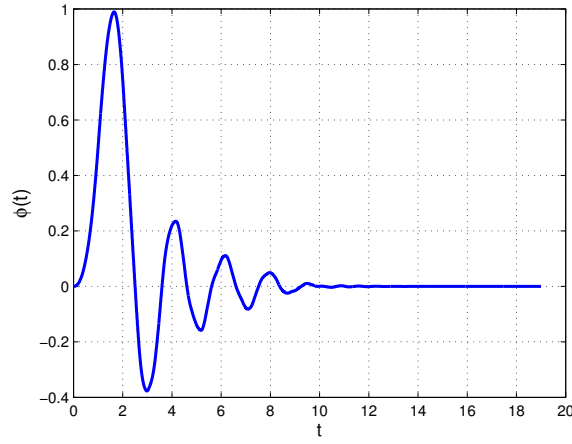
$$L = 20$$

$$\alpha = 1$$

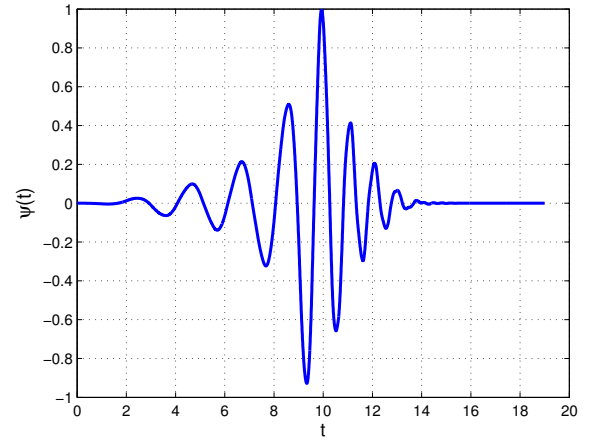
$$V = 6$$

In this example, we try to evaluate the role of  $\alpha$  on different properties of the design. In Ex. 3 we presented a purely frequency optimized ( $\alpha = 0$ ) filter bank, however in this example, we design purely time optimized ( $\alpha = 1$ ) filter bank. All the other parameters are same as in Ex. 3 except  $\alpha$ , which is unity in the present case. The discontinuities in the scaling and wavelet function can be seen in Fig. 4.3c and 4.3d respectively. The frequency response is shown in Fig. 4.3a, as the time variance is minimum for the present design, the frequency response gets crude. The time localization optimized filter banks as in present example could be useful in detecting the hidden discontinuities in the signals, as in the applications like image edge detection.

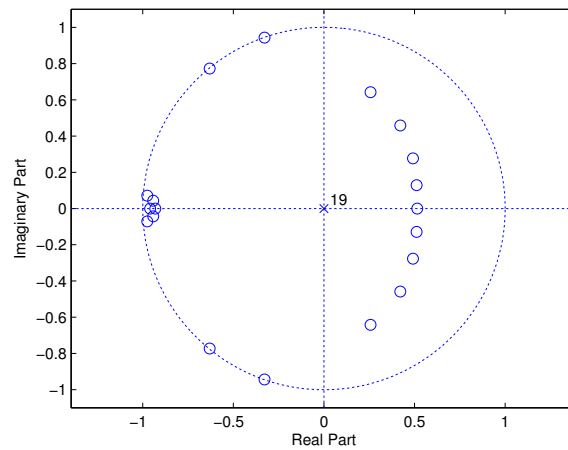


(a) Plot of  $|H_0(\omega)|$  and  $|H_1(\omega)|$  for Example-3(b) Plot of  $R(\omega)$  and  $R(\omega + \pi)$  for Example-3

(c) Analysis Scaling Function for Example-3

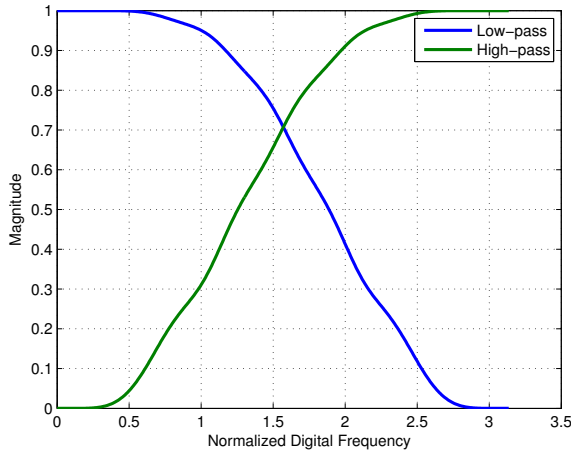
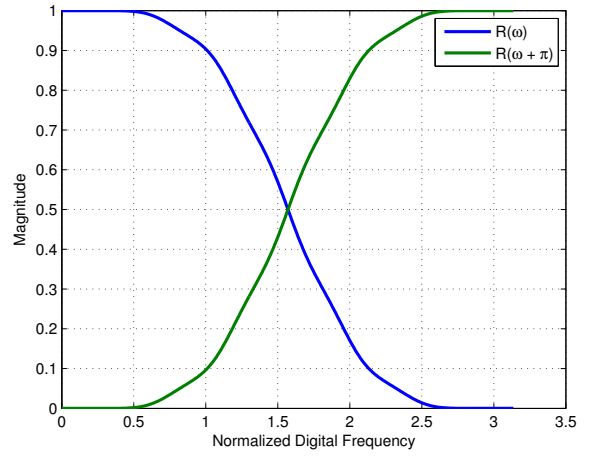
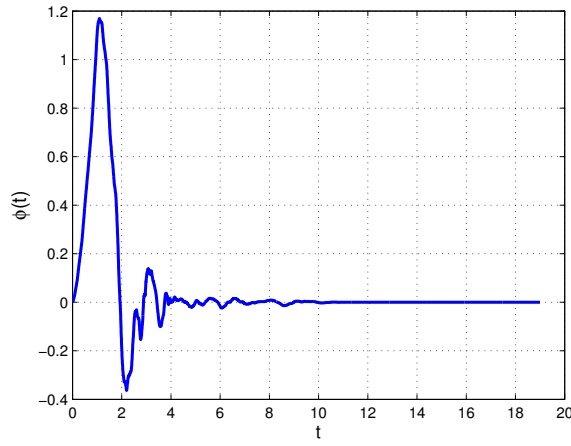


(d) Analysis Wavelet for Example-3

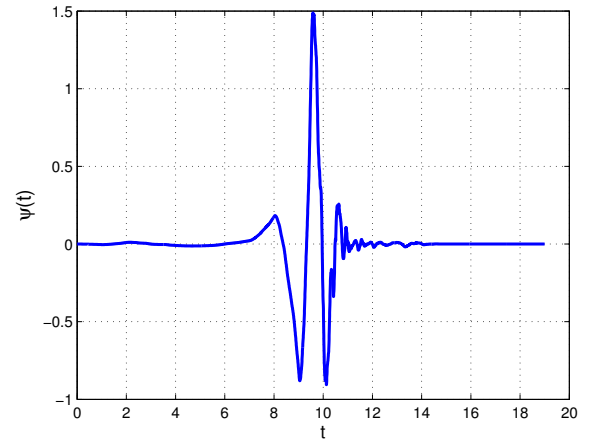


(e) Pole Zero Plot for Example-3

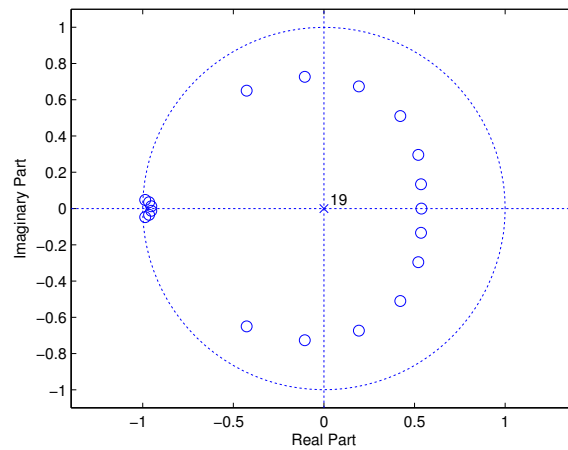
Figure 4.3: Example 3

(a) Plot of  $|H_0(\omega)|$  and  $|H_1(\omega)|$  for Example-4(b) Plot of  $R(\omega)$  and  $R(\omega + \pi)$  for Example-4

(c) Analysis Scaling Function for Example-4



(d) Analysis Wavelet for Example-4



(e) Pole Zero Plot for Example-4

Figure 4.4: Example 4

### 4.1.5 Design Example 5

**Parameters Taken:**

$$L = 20$$

$$\alpha = 0.5$$

$$V = 6$$

In this example, we changed  $\alpha$  to 0.5, hence we are in the midway of Ex. 3 and Ex. 4. The plots for the design examples are given in Fig. 4.5. Not much difference can be seen in the plots of the present example and Ex. 4, however the time-frequency localization measures of the present design are better than that of Ex. 4.

## 4.2 Design Examples for Design Problem 2 and 3

In this section, we present three examples, in which we try to reproduce the results obtained in the Sec. 4.1. Examples 6 and 7 are the solution of Design Problem 2, whereas Example 8 is the solution to the Design Problem 3. The different design problems are explained in the Sec. 3.8 of chapter 3. The time-frequency localization measures of analysis and synthesis low-pass filters of Example 2, 6, 8 and Example 3 and 5 are shown in Fig. 4.8.

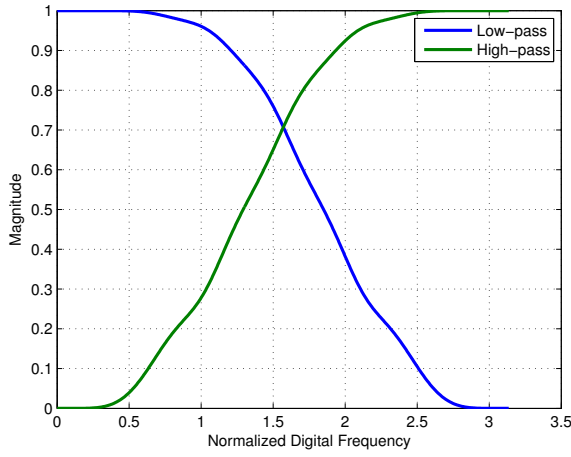
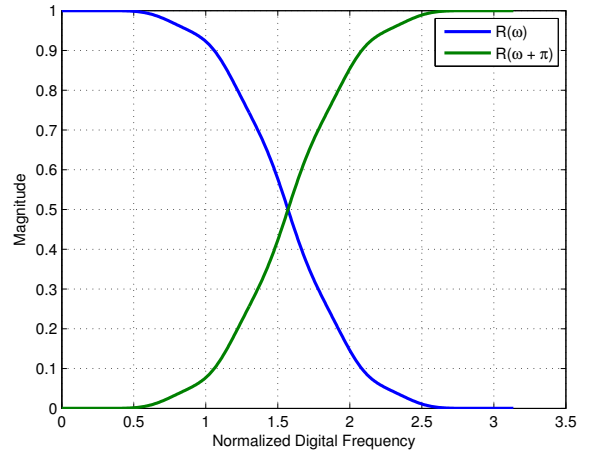
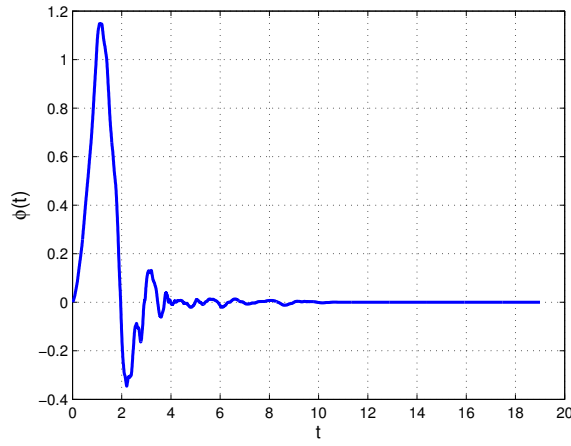
### 4.2.1 Design Example 6

**Parameters Taken:**

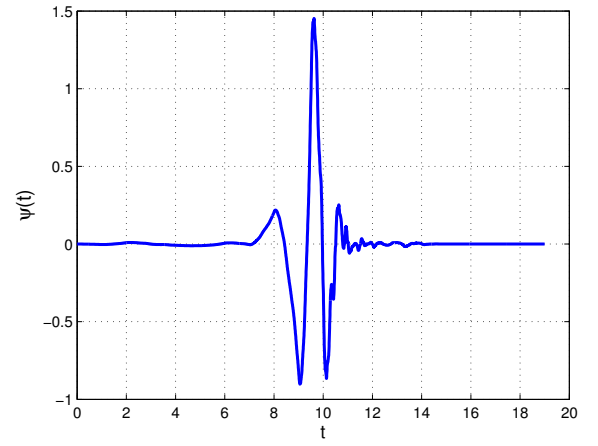
$$L = 12$$

$$\sigma_{\omega}^2 = 1.1396$$

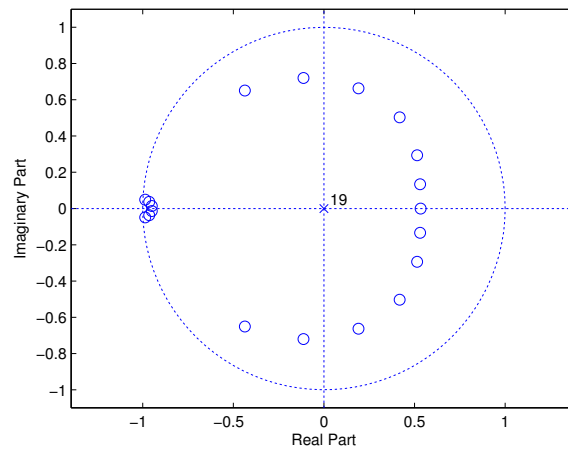
$$V = 2$$

(a) Plot of  $|H_0(\omega)|$  and  $|H_1(\omega)|$  for Example-5(b) Plot of  $R(\omega)$  and  $R(\omega + \pi)$  for Example-5

(c) Analysis Scaling Function for Example-4



(d) Analysis Wavelet for Example-4



(e) Pole Zero Plot for Example-5

Figure 4.5: Example 5

In this example, we try to reproduce the results obtained in Ex. 2. The frequency variance in Example 2 was obtained to be 1.1396. We fix the frequency variance to the same value and solve the Design Problem 2, after taking  $L = 12$  and  $V = 2$  as in Ex. 2. The time-frequency measures obtained for this example are almost same to that obtained in Ex. 2, which can be seen in Fig. 4.8. The different plots for this design example are shown in Fig. 4.6, the plots look similar to that of Ex. 2.

### 4.2.2 Design Example 7

**Parameters Taken:**

$$L = 20$$

$$\sigma_{\omega}^2 = 0.9876$$

$$V = 6$$

In this example, we try to reproduce the results obtained in Example 5. The frequency variance obtained in Example 5 was 0.9876, we fix the frequency variance to 0.9876 along with  $L = 20$  and  $V = 6$  and solve the Design Problem 2. Almost similar time-frequency localization measures are obtained which are shown in Fig. 4.8. The different plots of the present example are shown in Fig. 4.7 which look similar to the plots of Ex. 5.

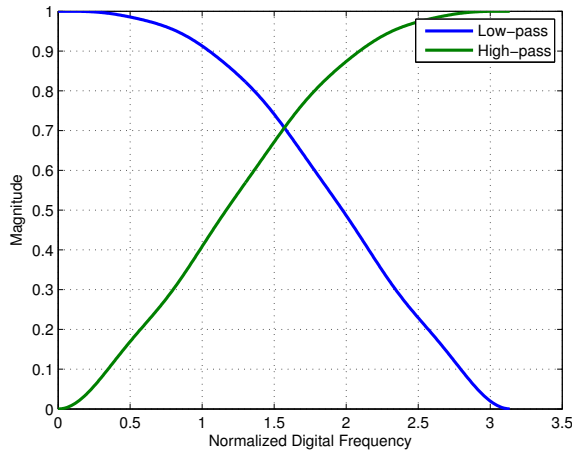
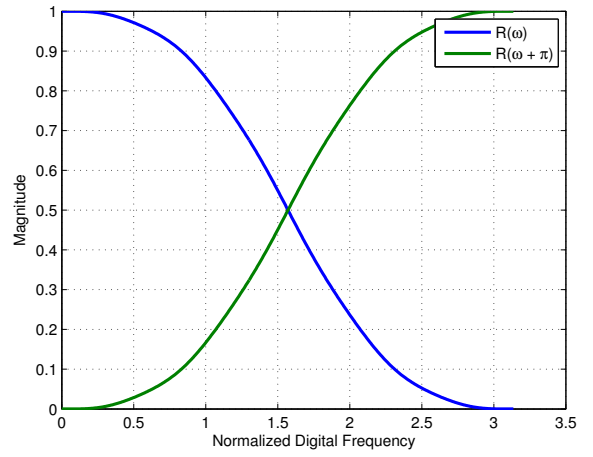
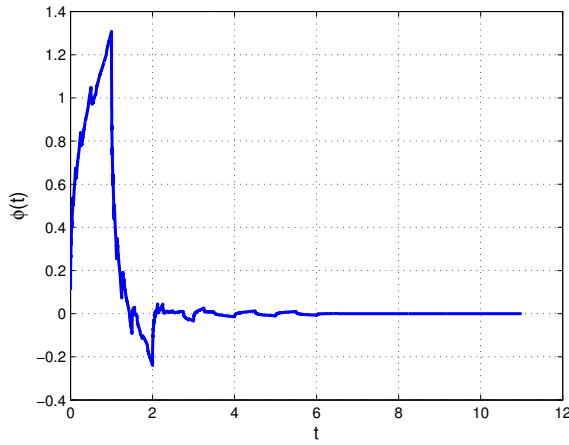
### 4.2.3 Design Example 8

**Parameters Taken:**

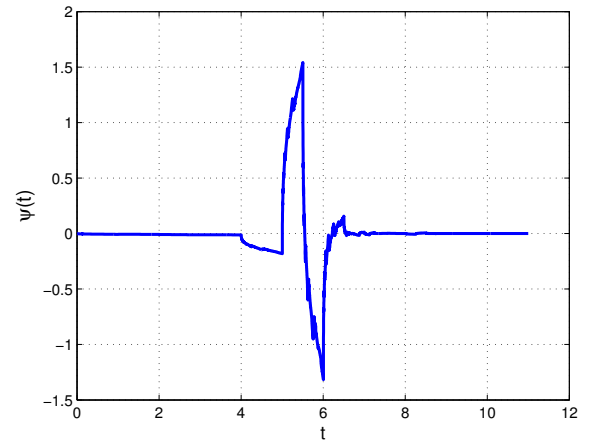
$$L = 12$$

$$\sigma_n^2 = 1.1396$$

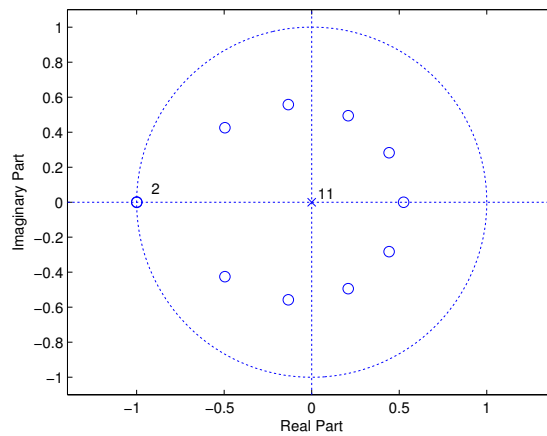
$$V = 2$$

(a) Plot of  $|H_0(\omega)|$  and  $|H_1(\omega)|$  for Example-6(b) Plot of  $R(\omega)$  and  $R(\omega + \pi)$  for Example-6

(c) Analysis Scaling Function for Example-6

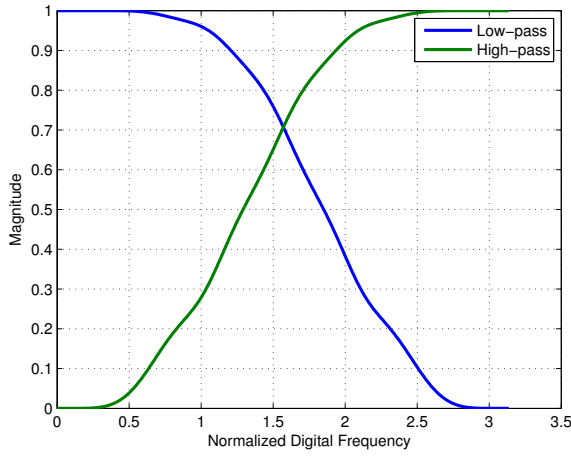
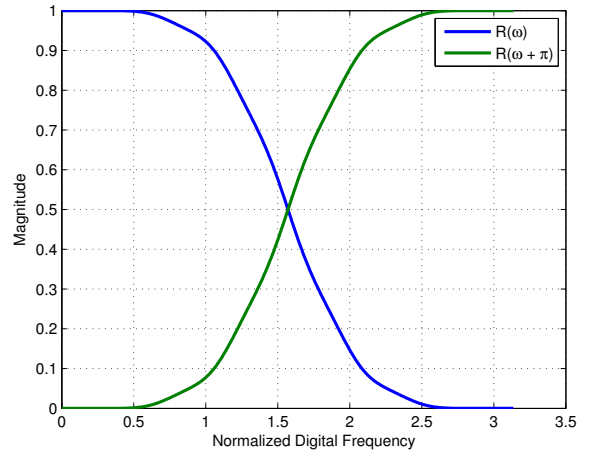
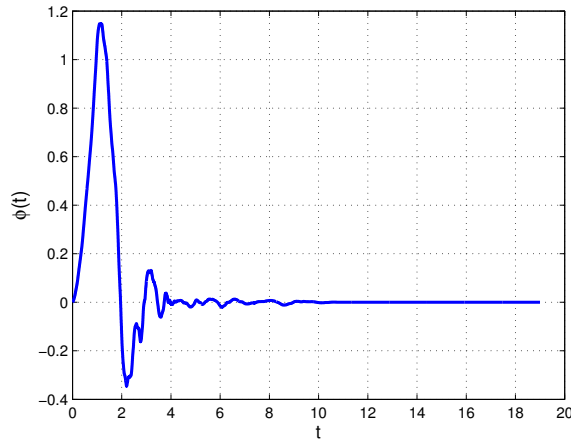


(d) Analysis Wavelet for Example-6

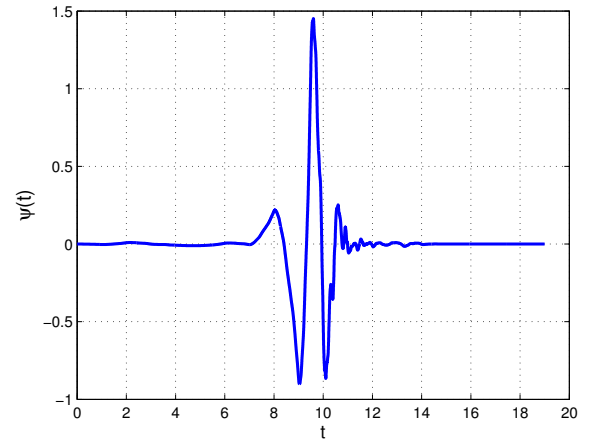


(e) Pole Zero Plot for Example-6

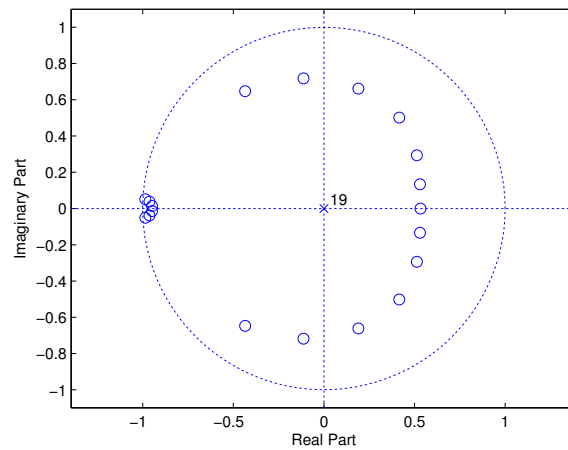
Figure 4.6: Example 6

(a) Plot of  $|H_0(\omega)|$  and  $|H_1(\omega)|$  for Example-7(b) Plot of  $R(\omega)$  and  $R(\omega + \pi)$  for Example-7

(c) Analysis Scaling Function for Example-7



(d) Analysis Wavelet for Example-7



(e) Pole Zero Plot for Example-7

Figure 4.7: Example 7

In this example, we solve the Design Problem 3 to reproduce the results of Example 2. In solving Design Problem 3, we first fix the time variance and then we solve the problem. The time variance obtained in Ex. 2 was 1.1396. We fixed the time variance to 1.1396,  $L = 12$  and  $V = 2$  and solve the problem. The plots (Fig. 4.9) obtained in the design are similar to the plots of Example 2 and 6. The time-frequency localization measures for the Examples 2, 6 and 8 are shown in Fig. 4.8.

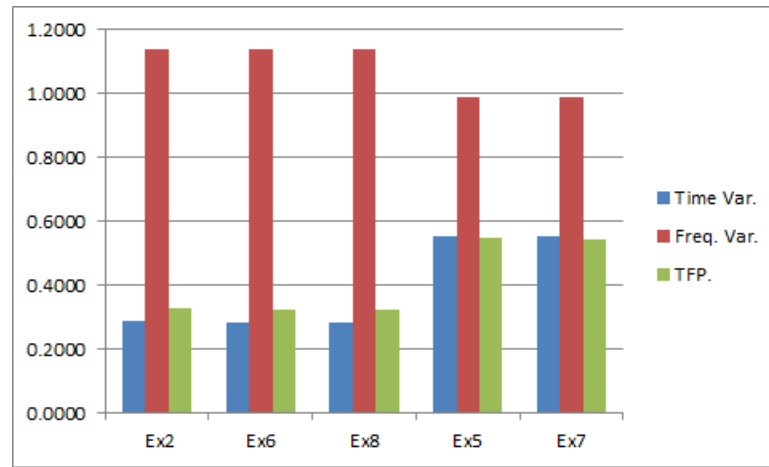
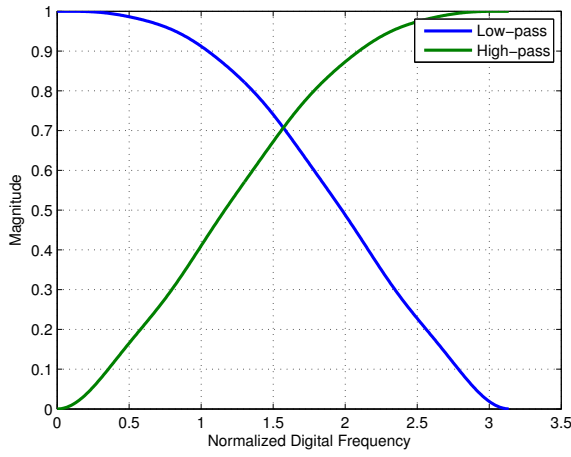
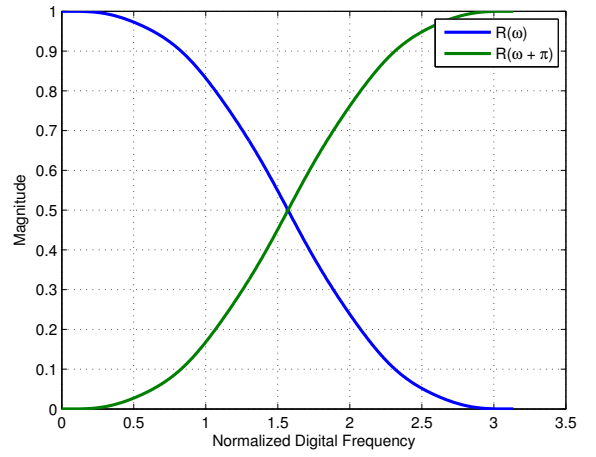
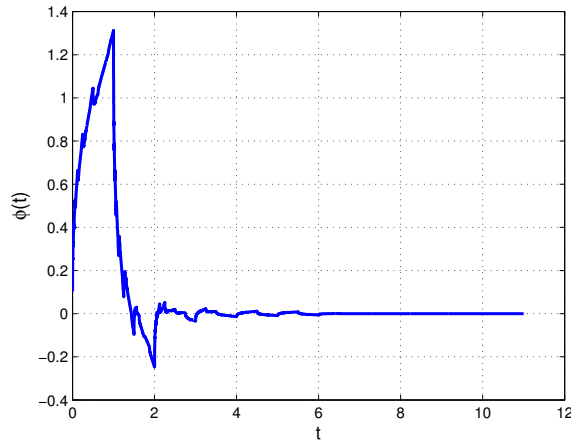
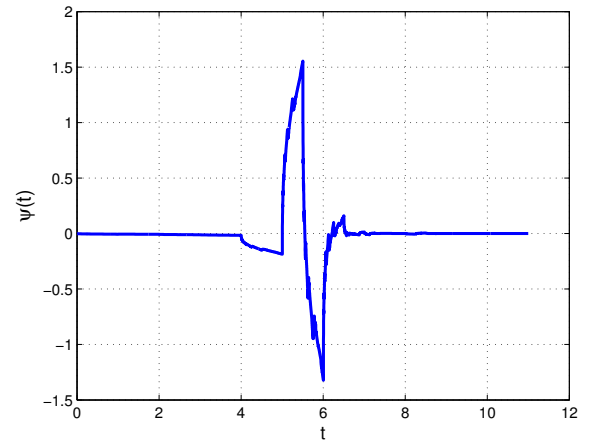


Figure 4.8: Time-Frequency Localization Measures.

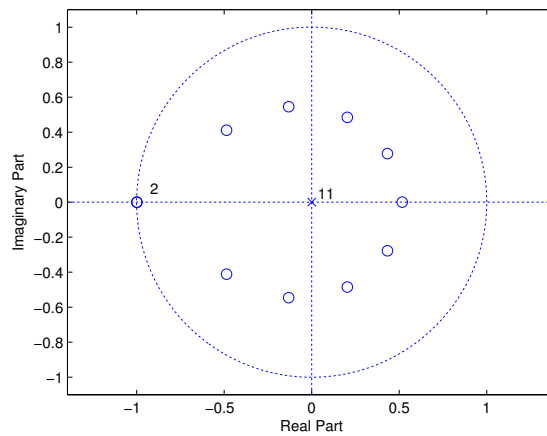


(a) Plot of  $|H_0(\omega)|$  and  $|H_1(\omega)|$  for Example-8(b) Plot of  $R(\omega)$  and  $R(\omega + \pi)$  for Example-8

(c) Analysis Scaling Function for Example-8



(d) Analysis Wavelet for Example-8



(e) Pole Zero Plot for Example-8

Figure 4.9: Example 8

### 4.3 Time-Frequency properties of obtained filters

In this section, we discuss the time-frequency properties of the filter banks obtained in the different design examples. In the proposed design approaches, we try to optimize the time variance and the frequency variance of the impulse response of the analysis filter, that is given by the following two equations respectively.

$$\begin{aligned}\sigma_n^2 &= \sum_n (n - n_0)^2 |h(n)|^2 \\ \sigma_\omega^2 &= \int_0^\pi \omega^2 |H(\omega)|^2 \frac{d\omega}{\pi}\end{aligned}$$

Where  $H(\omega)$  is DTFT of  $h(n)$  and

$$\begin{aligned}E &= \sum_n |h(n)|^2 \\ &= \frac{1}{2\pi} \int_{-\pi}^\pi |H(\omega)|^2 d\omega = 1\end{aligned}$$

and

$$n_0 = \sum_n n |h(n)|^2$$

The analysis low-pass and high-pass filter coefficients of the Design Examples 1, 2 and 6, 8 are tabulated in Table 4.3 and 4.2 respectively. The impulse response of the high-pass filter is given by the following equation,

$$h_1(n) = (-1)^n h_0(M - n)$$

The coefficients of the analysis low-pass filters of the Design Example 3, 4, 5 and 7 are tabulated in Table 4.4. After obtaining the filter coefficients, time and frequency variances are calculated along with the time-frequency product. It must be noted that the impulse response of the synthesis low-pass filter is flipped version of the impulse response of the analysis low-pass filter. Hence the analysis and the

Table 4.1: Time-Frequency properties of the analysis and synthesis LPF of Design Examples

	Ex. 1	Ex. 2	Ex. 3	Ex. 4	Ex. 5	Ex. 6	Ex. 7	Ex. 8
<b>Time Var.</b>	0.9123	0.2863	2.9453	0.5476	0.5536	0.2856	0.5518	0.2855
<b>Freq. Var.</b>	0.9056	1.1396	0.8408	1.0144	0.9876	1.1396	0.9876	1.1394
<b>TFP</b>	0.8262	0.3262	2.4764	0.5554	0.5468	0.3254	0.5450	0.3253

synthesis low-pass filter have equal time frequency measures. The time-frequency localization measures of the analysis and synthesis low-pass filters of all the design examples are tabulated in Table 4.1.

The time variance for Design Example 1 is larger than that of Ex. 2, 6 and 8, the reason is the number of vanishing moments, which is 6 in Ex. 1 and 2 in the remaining examples. In other words, design example 1 has less degrees of freedom to minimize the objective function. It can also be observed that the time variance of the Ex. 3 is larger than the others, the reason is that the value of  $\alpha$  was set to 0, i.e. the frequency variance was minimized only. It should be noted that the frequency variances of the filter impulse response for Ex. 2, 6 and 8 are similar. It is important to note that the frequency spread for Ex. 3 is smallest. In Ex. 3 only frequency variance was minimized, and hence the spread of the filter is smallest.

Table 4.2: Filter Coefficients of Design Examples

	Example 6		Example 8	
$n$	$h_0(n)$	$h_1(n)$	$h_0(n)$	$h_1(n)$
0	0.567241822046	-0.003300612963	0.563354783304	-0.002708168316
1	0.811398939993	-0.004721291265	0.813447649375	-0.003910418827
2	0.113515324092	-0.004822740050	0.116545961910	-0.004200379824
3	-0.081603088767	-0.005478945526	-0.083549160508	-0.004854454888
4	0.008374909878	-0.006767688996	0.010957266389	-0.006395484807
5	-0.007798917183	-0.007775377533	-0.009489541139	-0.007485762275
6	0.007775377533	-0.007798917183	0.007485762275	-0.009489541139
7	-0.006767688996	-0.008374909878	-0.006395484807	-0.010957266389
8	0.005478945526	-0.081603088767	0.004854454888	-0.083549160508
9	-0.004822740050	-0.113515324092	-0.004200379824	-0.116545961910
10	0.004721291265	0.811398939993	0.003910418827	0.813447649375
11	-0.003300612963	-0.567241822046	-0.002708168316	-0.563354783304

Table 4.3: Filter Coefficients of Design Examples

	Example 1		Example 2	
$n$	$h_0(n)$	$h_1(n)$	$h_0(n)$	$h_1(n)$
0	0.132185728555	-0.000909046447	0.571182784311	-0.003930240012
1	0.541299247393	-0.003722536272	0.809228936379	-0.005568206942
2	0.743596109666	0.002091614805	0.110662346640	-0.005446359196
3	0.243120202786	0.027833909285	-0.079741449148	-0.006088694678
4	-0.241455985037	0.015138742799	0.005597719251	-0.007088871255
5	-0.093634092804	-0.096892413669	-0.005916165924	-0.008007959709
6	0.096892413669	-0.093634092804	0.008007959709	-0.005916165924
7	0.015138742799	0.241455985037	-0.007088871255	-0.005597719251
8	-0.027833909285	0.243120202786	0.006088694678	-0.079741449148
9	0.002091614805	-0.743596109666	-0.005446359196	-0.110662346640
10	0.003722536272	0.541299247393	0.005568206942	0.809228936379
11	-0.000909046447	-0.132185728555	-0.003930240012	-0.571182784311

Table 4.4: Filter Coefficients of Design Examples

	Example 3	Example 4	Example 5	Example 7
$n$	$h_0(n)$	$h_0(n)$	$h_0(n)$	$h_0(n)$
0	0.134853752488	0.251649832525	0.241971496065	0.241998903060
1	0.507485955254	0.752618197767	0.738963866138	0.738868608303
2	0.697620208685	0.584864980916	0.604854444691	0.604921368095
3	0.335544432762	-0.094621416917	-0.071940007498	-0.071828747896
4	-0.163106499286	-0.124894408497	-0.148179777200	-0.148366027602
5	-0.228954331660	0.055082807763	0.046107911195	0.046459821737
6	0.058567353200	-0.015031543262	0.002938272940	0.002687998288
7	0.151739183957	0.006470637966	0.003744942074	0.003219754820
8	-0.031882272687	0.000016548419	-0.003817015232	-0.003144224454
9	-0.098455971926	-0.006475880465	-0.004254668772	-0.004373140808
10	0.018450619104	0.008397933982	0.007302506893	0.007149225792
11	0.070333766588	-0.008601037517	-0.007536277281	-0.007250630322
12	-0.021404340886	0.006325779751	0.005633752521	0.005354849366
13	-0.044272886618	-0.002395363828	-0.002646836610	-0.002458461179
14	0.025856534435	-0.000080125828	0.000139170987	0.000060100694
15	0.014400503472	0.005742064518	0.005370513478	0.005148994934
16	-0.015069934814	-0.006703710664	-0.006000915941	-0.005723285589
17	0.000141993280	0.000143203721	0.000038902642	0.000030552142
18	0.003221558739	0.002561560445	0.002264923761	0.002167970260
19	-0.000856061714	-0.000856498421	-0.000741642478	-0.000710067270

## Chapter 5

# Conclusion and Future Work

In the present work, a new framework to design the time-frequency localization optimized two-channel wavelet filter banks has been devised. In the devised framework, the prescribed number of vanishing moments ( $V < \frac{L}{2}$ ) can be achieved. We formulated a non-convex problem into a convex problem using trace parameterization of the quadratic forms. Three design problems have been proposed to design the time-frequency optimized filter banks. We discussed 8 design examples from all the three design problems, with different input parameters to investigate the role and effectiveness of each parameter and the design methodology.

The three design problems proposed in the present work are convex in matrix  $\mathbf{X}$ , from which we compute the autocorrelation function followed by the computation of analysis low-pass filter coefficients using the spectral factorization, which may or may not give the optimal filter. Approaches to find the optimal filter from the optimal matrix  $\mathbf{X}^{\text{opt}}$  can be further investigated and devised.

The trade-offs among the different input parameters to the proposed design problems can be further investigated. The effect of time-frequency localization on the frequency response parameters like roll-off factor, pass-band ripples can be further extended.

In the proposed work, the objective function was taken to be CCTFV, time variance and/ or the frequency variance of the analysis low-pass filter. The time-

frequency measures for corresponding analysis wavelets can also be taken as the design optimality criterion to design the filter banks.

Kha [10] et al. designed symmetric orthogonal complex valued filter banks, the proposed orthogonal design can be extended to the design of complex valued orthogonal filter banks.

# Bibliography

- [1] Ernst Breitenberger. Uncertainty measures and uncertainty relations for angle observables. *Foundations of physics*, 15(3):353–364, 1985.
- [2] David L Donoho and Philip B Stark. Uncertainty principles and signal recovery. *SIAM Journal on Appl. Math.*, 49(3):906–931, 1989.
- [3] B. Dumitrescu. *Positive Trigonometric Polynomials and Signal Processing Applications*. Springer Publishing Company, Incorporated, 2007.
- [4] B. Dumitrescu and Corneliu Popeea. Accurate computation of compaction filters with high regularity. *Signal Processing Letters, IEEE*, 9(9):278–281, Sept 2002.
- [5] D. Gabor. Theory of communication. *Proc. Inst. Elec. Eng.*, 93(26):429–441, 1946.
- [6] Michael Grant and Stephen Boyd. CVX: Matlab software for disciplined convex programming, version 2.1. <http://cvxr.com/cvx>, March 2014.
- [7] Richard A. Haddad, Ali N. Akansu, and Adil Benyassine. Time-frequency localization in transforms, subbands, and wavelets: a critical review. *Optical Engineering*, 32(7):1411–1429, 1993.
- [8] R. Ishii and K. Furukawa. The uncertainty principle in discrete signals. *IEEE Trans. Circ. Syst.*, 33(10):1032–1034, 1986.



- [9] A. Karmakar, A. Kumar, and R.K. Patney. Design of an optimal two-channel orthogonal filterbank using semidefinite programming. *Signal Processing Letters, IEEE*, 14(10):692–694, Oct 2007.
- [10] Ha Hoang Kha, Hoang Duong Tuan, Ba-Ngu Vo, and Truong Q. Nguyen. Symmetric orthogonal complex-valued filter bank design by semidefinite programming. In *ICASSP (3)*, pages 221–224, 2006.
- [11] Zhi-Quan Luo, Wing-Kin Ma, A.M.-C. So, Yinyu Ye, and Shuzhong Zhang. Semidefinite relaxation of quadratic optimization problems. *Signal Processing Magazine, IEEE*, 27(3):20–34, May 2010.
- [12] D.M. Monro and B. G. Sherlock. Space-frequency balance in biorthogonal wavelets. In *Int. Conf. Image Process., 1997. Proc.*, volume 1, pages 624–627 vol.1, 1997.
- [13] Joel M. Morris and Ravindra Peravali. Optimum duration discrete-time wavelets. *Optical Engineering*, 36(4):1241–1248, 1997.
- [14] Joel M. Morris and Ravindra Peravali. Minimum-bandwidth discrete-time wavelets. *Signal Process.*, 76(2):181–193, July 1999.
- [15] Joel M Morris and Hui Xie. Minimum duration-bandwidth discrete-time wavelets. *Optical Engineering*, 35(7):2075–2078, 1996.
- [16] Reza Parhizkar, Yann Barbotin, and Martin Vetterli. Sequences with minimal time-frequency uncertainty. *arXiv preprint arXiv:1302.2082*, 2013.
- [17] T. Przebinda, V. DeBrunner, and M. Ozaydin. Using a new uncertainty measure to determine optimal bases for signal representations. In *Proc. IEEE Int. Conf. Acoust. Speech Signal Process. ICASSP '99*, volume 3, pages 1365–1368 vol.3, 1999.

- [18] M. Sharma, V.M. Gadre, and S. Porwal. An eigenfilter based approach to the design of time-frequency localization optimized two-channel linear phase biorthogonal filter banks. Submitted.
- [19] Lixin Shen and Zuowei Shen. Compression with time-frequency localization filters. *Wavelets and Splines, Athens*, pages 428–443, 2006.
- [20] D. Slepian. Prolate spheroidal wave functions, fourier analysis, and uncertainty. V - The discrete case. *Bell System Tech. Journal*, 57:1371–1430, June 1978.
- [21] G. Strang and T. Nguyen. *Wavelets and Filter Banks*. Wellesley-Cambridge Press, 1996.
- [22] Gilbert Strang. Eigenvalues of  $(\downarrow 2)$  H and convergence of the cascade algorithm. *Signal Processing, IEEE Transactions on*, 44(2):233–238, 1996.
- [23] David B.H. Tay. Balanced-uncertainty optimized wavelet filters with prescribed regularity. In *Proc. IEEE Int. Symp. Circ. Syst. ISCAS '99.*, volume 3, pages 532–535 vol.3, 1999.
- [24] David B.H. Tay. Balanced-uncertainty optimized wavelet filters with prescribed vanishing moments. *Circ. Syst. and Signal Process.*, 23(2):105–121, 2004.
- [25] T. Przebinda V. DeBrunner, J. P. Havlicek and M. Ozaydin. Entropy-based uncertainty measures for  $l^2(\mathbb{R}^n)$ ,  $l^2(\mathbb{Z})$ , and  $l^2(\mathbb{Z}/n\mathbb{Z})$  with a hirschman optimal transform for  $l^2(\mathbb{Z}/n\mathbb{Z})$ . *IEEE Trans. Signal Process.*, 53(8):2690–2699, 2005.
- [26] P.P. Vaidyanathan and P.-Q. Hoang. Lattice structures for optimal design and robust implementation of two-channel perfect-reconstruction QMF banks. *IEEE Trans. Acoust. Speech Signal Process.*, 36(1):81–94, 1988.

- [27] Lieven Vandenberghe and Stephen Boyd. Semidefinite programming. *SIAM Review*, 38(1):49–95, 1996.
- [28] Y.V. Venkatesh, S. Kumar Raja, and G.V. Sagar. On bandlimited signals with minimal space/time-bandwidth product. In *Multimedia and Expo, 2004. ICME '04. 2004 IEEE International Conference on*, volume 3, pages 1911–1914 Vol.3, June 2004.
- [29] M. Vetterli and C. Herley. Wavelets and filter banks: theory and design. *IEEE Trans. Signal. Process.*, 40(9):2207–2232, September 1992.
- [30] Jie Yan and Wu-Sheng Lu. Towards global design of orthogonal filter banks and wavelets. *Electrical and Computer Engineering, Canadian Journal of*, 34(4):145–151, Fall 2009.
- [31] Jian-Kang Zhang, T.N. Davidson, and Kon Max Wong. Efficient design of orthonormal wavelet bases for signal representation. *Signal Processing, IEEE Transactions on*, 52(7):1983–1996, July 2004.

# Appendices

# Appendix A

## A.1 Derivation of Matrix Formulation for Frequency Variance

Equation 3.19 has been derived in this section. The DTFT of the  $h(n) \in l^2(\mathbb{Z})$

$$H(\omega) = \sum_{n=0}^M h(n)e^{-j\omega n} \quad (\text{A.1})$$

Recall,

$$h(n) = 0, \forall n \in \{(n < 0) \cup (n > M)\}$$

The DTFT of  $h(n)$  can be rewritten in matrix form as:

$$H(\omega) = \mathbf{h}^T \mathbf{e}(\omega) \quad (\text{A.2})$$

where,

$$\mathbf{e}(\omega) = [e^{-j\omega} \quad e^{-j\omega 1} \quad e^{-j\omega 2} \quad \dots \quad e^{-j\omega M}]^T \quad (\text{A.3})$$

The frequency variance  $\sigma_\omega^2$  is given by

$$\sigma_\omega^2 = \frac{1}{\pi} \int_0^\pi \omega^2 |H(\omega)| d\omega \quad (\text{A.4})$$

$$= \frac{1}{\pi} \int_0^\pi \omega^2 \{\mathbf{h}^T \mathbf{e}(\omega) \mathbf{e}^H(\omega) \mathbf{h}\} d\omega \quad (\text{A.5})$$

$$= \mathbf{h}^T \left\{ \int_0^\pi \omega^2 \mathbf{e}(\omega) \mathbf{e}^H(\omega) \frac{d\omega}{\pi} \right\} \mathbf{h} \quad (\text{A.6})$$

$$= \mathbf{h}^T \left\{ \int_0^\pi \omega^2 \mathbf{E}(\omega) \frac{d\omega}{\pi} \right\} \mathbf{h} \quad (\text{A.7})$$

$$= \mathbf{h}^T \mathbf{F} \mathbf{h} \quad (\text{A.8})$$

where,

$$\mathbf{F} = \int_0^\pi \omega^2 \mathbf{E}(\omega) \frac{d\omega}{\pi} \quad (\text{A.9})$$

and

$$\mathbf{E}(\omega) = \begin{bmatrix} e^{-j\omega 0} \\ e^{-j\omega 1} \\ \vdots \\ e^{-j\omega M} \end{bmatrix} \begin{bmatrix} e^{j\omega 0} & e^{j\omega 1} & \dots & e^{j\omega M} \end{bmatrix} \quad (\text{A.10})$$

$$= \begin{bmatrix} 1 & e^{j\omega 1} & e^{j\omega 2} & \dots & e^{j\omega M} \\ e^{-j\omega 1} & 1 & e^{j\omega 1} & \dots & e^{j\omega(M-1)} \\ e^{-j\omega 2} & e^{-j\omega 1} & 1 & \dots & e^{j\omega(M-2)} \\ \vdots & \vdots & \vdots & \ddots & \vdots \\ e^{-j\omega M} & e^{-j\omega(M-1)} & e^{-j\omega(M-2)} & \dots & 1 \end{bmatrix} \quad (\text{A.11})$$

The element of the  $\mathbf{E}$  matrix is  $E_{k,l} = e^{j\omega(l-k)}$ . So when  $k = l$  the element at that place is 1 which means all the diagonal elements are 1.

Now consider the integral

$$\frac{1}{\pi} \int_0^\pi \omega^2 e^{j\omega p} d\omega$$

For  $p=0$ ,

$$\frac{1}{\pi} \int_0^\pi \omega^2 e^{j\omega p} d\omega = \frac{1}{\pi} \int_0^\pi \omega^2 d\omega = \frac{\omega^3}{3\pi} \Big|_0^\pi = \frac{\pi^2}{3}. \quad (\text{A.12})$$

For  $p > 0$ ,

$$\begin{aligned} \frac{1}{\pi} \int_0^\pi \omega^2 e^{j\omega p} d\omega &= \frac{\omega^2 e^{j\omega p}}{jp} \Big|_0^\pi - \int_0^\pi \frac{2\omega e^{j\omega p}}{jp} d\omega \\ &= \frac{\omega^2 e^{j\omega p}}{jp} \Big|_0^\pi - \frac{2}{jp} \int_0^\pi \omega e^{j\omega p} d\omega \\ &= \frac{\omega^2 e^{j\omega p}}{jp} \Big|_0^\pi - \frac{2}{jp} \left\{ \frac{\omega e^{j\omega p}}{jp} \Big|_0^\pi - \int_0^\pi \frac{e^{j\omega p}}{jp} d\omega \right\} \\ &= \frac{\omega^2 e^{j\omega p}}{jp} \Big|_0^\pi - \frac{2}{(jp)^2} \left\{ \omega e^{j\omega p} - \frac{e^{j\omega p}}{jp} \right\} \Big|_0^\pi \\ &= \frac{\omega^2 e^{j\omega p}}{jp} \Big|_0^\pi + \frac{2}{(p)^2} \left\{ \omega e^{j\omega p} - \frac{e^{j\omega p}}{jp} \right\} \Big|_0^\pi \\ &= \frac{\pi^2(-1)^p}{jp} + \frac{2}{p^2} \left\{ \pi e^{j\pi p} - \frac{e^{j\pi p}}{jp} \right\} - \left[ 0 + \frac{2}{p^2} \left( \frac{-1}{jp} \right) \right] \end{aligned}$$

Hence for  $p > 0$ ,

$$\frac{1}{\pi} \int_0^\pi \omega^2 e^{j\omega p} d\omega = \frac{\pi^2(-1)^p}{jp} + \frac{2\pi(-1)^p}{p^2} - \frac{2(-1)^p}{jp^3} + \frac{2}{jp^3} \quad (\text{A.13})$$

From expressions A.9, A.11, A.12 and A.13, we can evaluate the  $\mathbf{F}$  matrix. The expression for the  $\mathbf{F}$  matrix is given below.

$$\mathbf{F}_{\mathbf{k},\mathbf{l}} = \begin{cases} \frac{\pi^2}{3} & \text{if } k = l \\ \frac{\pi^2(-1)^{(l-k)}}{j(l-k)} + \frac{2\pi(-1)^{(l-k)}}{(l-k)^2} + \frac{2(1-(-1)^{(l-k)})}{j(l-k)^3} & \text{if } l \neq k \end{cases} \quad (\text{A.14})$$